Teuvo Kilpiö<sup>1</sup> / Vincenzo Russo<sup>2</sup> / Kari Eränen<sup>1</sup> / Tapio Salmi<sup>1</sup>

# Design and modeling of laboratory scale three-phase fixed bed reactors

- <sup>1</sup> Department of Chemical Engineering, PCC, Åbo Akademi, Fl-20500 Turku/Åbo, Finland, E-mail: teuvo.kilpio@abo.fi, kari.eranen@abo.fi, tsalmi@abo.fi
- <sup>2</sup> Chemical Sciences Department, University of Naples 'Federico II', IT-80126 Naples, Italy, E-mail: v.russo@unina.it

**DOI:** 10.1515/psr-2015-0020

### **Nomenclature**

$a_0, a_f$	Activity, initial, final	[]
	Area-to-volume ratio	$[m^2/m^3]$
L	Parameter	[]
-p	External surface area of particle	$[m^2]$
,	Specific surface area of particles	$[m^2/m^3]$
	Parameter	[]
i	Local concentration of component $i$ in liquid, $i = A, B, C, D, H$	[mol/l]
i.G	Concentration of component <i>i</i> in gas	[mol/l]
i,G i,L	Concentration of component $i$ in liquid, $i = A, B, C$	[mol/l]
i,F	Concentration of component <i>i</i> in the fluid phase	[mol/m <sup>3</sup> ]
rin i,F	Initial concentration of component $i$ in the fluid phase	[mol/m <sup>3</sup> ]
i,S	Concentration of component $i$ in the solid	[mol/m <sup>3</sup> ]
rin i,S	Initial concentration of component $i$ in the solid	[mol/m <sup>3</sup> ]
$c_{P,F}$ $c_{P,L}$	Specific heat of the fluid, liquid	[J/(kg K)]
P,S	Specific heat of the solid	[J/(kg K)]
A,B	Diffusivity of $A$ in solvent $B$	$[m^2/s]$
$D_{A,B}^{0},D_{B,A}^{0}$	Infinite dilution diffusivity of $A$ in $B$ and $B$ in $A$	$[m^2/s]$
$\mathcal{O}_{A,i}^0$	Infinite dilution diffusivity of $A$ in $i$	$[m^2/s]$
$O_{A,M}$	Diffusivity in mixture	$[m^2/s]$
) <sub>a,L</sub>	Axial dispersion coefficient in liquid	$[m^2/s]$
$O_{A,L}$	Diffusivity of component $A$ in liquid	$[m^2/s]$
) e,i	Effective diffusivity of the compound $i$ , $i = A$ , $B$ , $C$	$[m^2/s]$
$\mathbf{O}_{i,L}$	Diffusivity of component <i>i</i> in liquid	$[m^2/s]$
)r,F	Radial dispersion coefficient of the fluid	$[m^2/s]$
O <sub>z,F</sub>	Axial dispersion coefficient of the fluid	$[m^2/s]$
К	Krischer-Kast hydraulic diameter $d_k = d_p \sqrt[4]{\frac{16\varepsilon_b^3}{9\pi(1-\varepsilon_b)^2}}$	[m]
<sub>0</sub>	Particle diameter	[m]
$E_{1}^{0}$ , $E_{2}$	Ergun equation constants	[]
	Friction factor	[]
	Gravity constant	$[m^2/s]$

**Tapio Salmi** is the corresponding author.
© 2016 Walter de Gruyter GmbH, Berlin/Munich/Boston.
This content is free.

Automatically generated rough PDF by ProofCheck from River Valley Technologies Ltd

$Ga_G$ , $Ga_L$	Galileo number for gas and liquid	[]
Geo	Dimensionless geometry dependent	[]
	variable	
$H_{GL}$	Gas-liquid heat transfer rate	$[J/(m^3 s)]$
$h_w$	Wall heat transfer coefficient	$[W/(m^2 K)]$
i	Reaction rate order	[]
$J_{GL}$	Gas-liquid mass transfer rate	$[\text{mol}/(\text{m}^3 \text{ s})]$
$k, k_i$	Reaction rate constant, units to	[mol/(g s)]
,	express the rate, $j$ for reaction $j$	
$k_d$	Deactivation rate constant units to	[1/s]
	express the activation change	
$k_l$	Liquid-solid mass transfer coefficient	[1/s]
$k_{l}a$	Combined gas-liquid mass transfer	[1/s]
	coefficient	
$k_r$	Radial thermal conductivity	[W/(m K)]
$K_{i}$	Adsorption parameters for	[l/mol]
,	component $\hat{j} = A, B, C, H, K, L$	
$K_{eq}$	Equilibrium constant	[]
$L^{-\eta}$	Reactor length	[m]
M	Total number of volume elements	[]
$M_{\scriptscriptstyle B}$	Molar mass of solvent	[kg/kmol]
$m_L$	Mass flux of liquid	$[kg/m^2 s]$
n	Exponent	
$n_i$	Adsorption exponent for component <i>i</i>	
Nu	Nusselt number	[]
m	Exponent	[]
p	Pressure	[Pa]
$p_1, p_4, p_5$	Reaction rate constant, deactivation	
11/14/13	rate constant and final activity in	
	Figure 13–Figure 17	
Pe	Peclet number	[]
r	Radial location, in particle or catalyst	[m]
	bed	
$r_i$	Reaction rate for component $i$ ; $i = A$ ,	[mol/(g s)]
•	В, С	- 0/-
		[mol/(g s)]
$r_{ij}$	Reaction rate of component i in	[11101/ (5 3)]
$r_{i,j}$	Reaction rate of component $i$ in reaction $j$	[111017 (g 3)]
		[mol/(g s)]
$r_{i,j}$ $r_{i,S}$	reaction <i>j</i> Reaction rate at the surface of the	_
$r_{i,S}$	reaction j	[mol/(g s)]
$r_{i,S}$ $r_{i,x}$	reaction <i>j</i> Reaction rate at the surface of the particle, <i>A</i> , <i>B</i> , <i>C</i>	[mol/(g s)] $[mol/(g s)]$
$r_{i,S}$	reaction $j$ Reaction rate at the surface of the particle, $A$ , $B$ , $C$ Reaction rate at location $x$	[mol/(g s)]
$egin{aligned} r_{i,S} \ r_{i,x} \ r_p \end{aligned}$	reaction <i>j</i> Reaction rate at the surface of the particle, <i>A</i> , <i>B</i> , <i>C</i> Reaction rate at location <i>x</i> Distance from the particle centre	[mol/(g s)] [mol/(g s)]
$egin{aligned} r_{i,S} \ r_{i,x} \ r_p \ R \ R_p \end{aligned}$	reaction $j$ Reaction rate at the surface of the particle, $A$ , $B$ , $C$ Reaction rate at location $x$ Distance from the particle centre Reactor radius	[mol/(g s)] [mol/(g s)] [ ] [m]
$egin{aligned} r_{i,S} \ r_{i,x} \ r_p \ R \end{aligned}$	reaction <i>j</i> Reaction rate at the surface of the particle, <i>A</i> , <i>B</i> , <i>C</i> Reaction rate at location <i>x</i> Distance from the particle centre Reactor radius Particle radius	[mol/(g s)] [mol/(g s)] [ ] [m] [m]
$r_{i,S}$ $r_{i,x}$ $r_{p}$ $R$ $R_{p}$ $R_{g}$	reaction <i>j</i> Reaction rate at the surface of the particle, <i>A</i> , <i>B</i> , <i>C</i> Reaction rate at location <i>x</i> Distance from the particle centre Reactor radius Particle radius Ideal gas constant	[mol/(g s)] [mol/(g s)] [ ] [m] [m] [m] [J/(mol K)]
$r_{i,S}$ $r_{i,x}$ $r_{p}$ $R$ $R_{p}$ $R_{g}$ $Re_{L}$	reaction <i>j</i> Reaction rate at the surface of the particle, <i>A</i> , <i>B</i> , <i>C</i> Reaction rate at location <i>x</i> Distance from the particle centre Reactor radius Particle radius Ideal gas constant Reynolds number of liquid	[mol/(g s)] [mol/(g s)] [ ] [m] [m] [m] [J/(mol K)]
$r_{i,S}$ $r_{i,x}$ $r_{p}$ $R$ $R_{P}$ $R_{g}$ $Re_{L}$ $Re_{G}$	reaction <i>j</i> Reaction rate at the surface of the particle, <i>A</i> , <i>B</i> , <i>C</i> Reaction rate at location <i>x</i> Distance from the particle centre Reactor radius Particle radius Ideal gas constant Reynolds number of liquid Reynolds number of gas	[mol/(g s)] [mol/(g s)] [ ] [m] [m] [J/(mol K)] [ ]
$r_{i,s}$ $r_{i,x}$ $r_{p}$ $R$ $R_{p}$ $R_{g}$ $Re_{L}$ $Re_{G}$ $s$	reaction <i>j</i> Reaction rate at the surface of the particle, <i>A</i> , <i>B</i> , <i>C</i> Reaction rate at location <i>x</i> Distance from the particle centre Reactor radius Particle radius Ideal gas constant Reynolds number of liquid Reynolds number of gas Surface shape factor	[mol/(g s)] [mol/(g s)] [ ] [m] [m] [J/(mol K)] [ ] [ ]
$r_{i,S}$ $r_{i,x}$ $r_{p}$ $R$ $R_{p}$ $R_{g}$ $Re_{L}$ $Re_{G}$ $S$ $Sc_{L}$	reaction <i>j</i> Reaction rate at the surface of the particle, <i>A</i> , <i>B</i> , <i>C</i> Reaction rate at location <i>x</i> Distance from the particle centre Reactor radius Particle radius Ideal gas constant Reynolds number of liquid Reynolds number of gas Surface shape factor Schmidt number of liquid	[mol/(g s)] [mol/(g s)] [ ] [m] [m] [J/(mol K)] [ ] [ ] [ ]
$r_{i,S}$ $r_{i,x}$ $r_{p}$ $R$ $R_{p}$ $R_{g}$ $Re_{L}$ $Re_{G}$ $S$ $Sc_{L}$ $Sh$ $T$ $T_{F}$	reaction <i>j</i> Reaction rate at the surface of the particle, <i>A</i> , <i>B</i> , <i>C</i> Reaction rate at location <i>x</i> Distance from the particle centre Reactor radius Particle radius Ideal gas constant Reynolds number of liquid Reynolds number of gas Surface shape factor Schmidt number of liquid Sherwood number	[mol/(g s)] [mol/(g s)] [] [m] [m] [J/(mol K)] [] [] [] []
$r_{i,S}$ $r_{i,x}$ $r_{p}$ $R$ $R_{p}$ $R_{g}$ $Re_{L}$ $Re_{G}$ $S$ $Sc_{L}$ $Sh$ $T$ $T_{F}$ $T_{F}^{INN}$	reaction <i>j</i> Reaction rate at the surface of the particle, <i>A</i> , <i>B</i> , <i>C</i> Reaction rate at location <i>x</i> Distance from the particle centre Reactor radius Particle radius Ideal gas constant Reynolds number of liquid Reynolds number of gas Surface shape factor Schmidt number of liquid Sherwood number Temperature	[mol/(g s)] [mol/(g s)] [] [m] [m] [J/(mol K)] [] [] [] [] [] [] [] [K]
$r_{i,S}$ $r_{i,x}$ $r_{p}$ $R$ $R_{p}$ $R_{g}$ $Re_{L}$ $Re_{G}$ $S$ $Sc_{L}$ $Sh$ $T$ $T_{F}$ $T_{F}^{IN}$ $T_{S}$	reaction <i>j</i> Reaction rate at the surface of the particle, <i>A</i> , <i>B</i> , <i>C</i> Reaction rate at location <i>x</i> Distance from the particle centre Reactor radius Particle radius Ideal gas constant Reynolds number of liquid Reynolds number of gas Surface shape factor Schmidt number of liquid Sherwood number Temperature Temperature of the fluid	[mol/(g s)] [mol/(g s)] [] [m] [m] [J/(mol K)] [] [] [] [] [] [] [K] [K]
$r_{i,S}$ $r_{i,x}$ $r_{p}$ $R$ $R_{p}$ $R_{g}$ $Re_{L}$ $Re_{G}$ $S$ $Sc_{L}$ $Sh$ $T$ $T_{F}$ $T_{F}^{INN}$	reaction <i>j</i> Reaction rate at the surface of the particle, <i>A</i> , <i>B</i> , <i>C</i> Reaction rate at location <i>x</i> Distance from the particle centre Reactor radius Particle radius Ideal gas constant Reynolds number of liquid Reynolds number of gas Surface shape factor Schmidt number of liquid Sherwood number Temperature Temperature of the fluid Initial temperature of the fluid	[mol/(g s)] [mol/(g s)] [] [m] [m] [J/(mol K)] [] [] [] [] [] [] [K] [K]
$r_{i,S}$ $r_{i,x}$ $r_{p}$ $R$ $R_{p}$ $R_{g}$ $Re_{L}$ $Re_{G}$ $S$ $Sc_{L}$ $Sh$ $T$ $T_{F}$ $T_{F}^{IN}$ $T_{S}$	reaction <i>j</i> Reaction rate at the surface of the particle, <i>A</i> , <i>B</i> , <i>C</i> Reaction rate at location <i>x</i> Distance from the particle centre Reactor radius Particle radius Ideal gas constant Reynolds number of liquid Reynolds number of gas Surface shape factor Schmidt number of liquid Sherwood number Temperature Temperature Temperature of the fluid Initial temperature of the solid	[mol/(g s)] [mol/(g s)] [] [m] [m] [J/(mol K)] [] [] [] [] [K] [K] [K] [K] [K]
$r_{i,S}$ $r_{i,x}$ $r_p$ $R$ $R_p$ $R_g$ $Re_L$ $Re_G$ $S$ $Sc_L$ $Sh$ $T$ $T_F$ $T_F^F$ $T_F^F$ $T_S^F$ $T_S^F$ $T_S^F$	reaction <i>j</i> Reaction rate at the surface of the particle, <i>A</i> , <i>B</i> , <i>C</i> Reaction rate at location <i>x</i> Distance from the particle centre Reactor radius Particle radius Ideal gas constant Reynolds number of liquid Reynolds number of gas Surface shape factor Schmidt number of liquid Sherwood number Temperature Temperature Temperature of the fluid Initial temperature of the solid Initial temperature of the solid	[mol/(g s)] [mol/(g s)] [] [m] [m] [J/(mol K)] [] [] [] [] [K] [K] [K] [K]
$r_{i,S}$ $r_{i,x}$ $r_p$ $R$ $R_P$ $R_g$ $Re_L$ $Re_G$ $S$ $Sc_L$ $Sh$ $T$ $T_F$ $T_F^{IN}$ $T_S^{IN}$ $T_w$	reaction <i>j</i> Reaction rate at the surface of the particle, <i>A</i> , <i>B</i> , <i>C</i> Reaction rate at location <i>x</i> Distance from the particle centre Reactor radius Particle radius Ideal gas constant Reynolds number of liquid Reynolds number of gas Surface shape factor Schmidt number of liquid Sherwood number Temperature Temperature of the fluid Initial temperature of the fluid Initial temperature of the solid Initial temperature of the solid	[mol/(g s)] [mol/(g s)] [] [m] [m] [J/(mol K)] [] [] [] [] [K] [K] [K] [K] [K]
$r_{i,S}$ $r_{i,x}$ $r_{p}$ $R$ $R_{p}$ $R_{g}$ $Re_{L}$ $Re_{G}$ $S$ $Sc_{L}$ $Sh$ $T$ $T_{F}$ $T_{S}$ $T_{S}$ $T_{S}$ $T_{w}$ $t$	reaction <i>j</i> Reaction rate at the surface of the particle, <i>A</i> , <i>B</i> , <i>C</i> Reaction rate at location <i>x</i> Distance from the particle centre Reactor radius Particle radius Ideal gas constant Reynolds number of liquid Reynolds number of gas Surface shape factor Schmidt number of liquid Sherwood number Temperature Temperature of the fluid Initial temperature of the fluid Initial temperature of the solid Initial temperature of the solid Temperature of the wall Time	[mol/(g s)] [mol/(g s)] [] [m] [m] [m] [J/(mol K)] [] [] [] [] [K] [K] [K] [K] [K] [K] [K
$r_{i,S}$ $r_{i,x}$ $r_{p}$ $R$ $R$ $R_{p}$ $R_{g}$ $Re_{L}$ $Re_{G}$ $S$ $Sc_{L}$ $Sh$ $T$ $T_{F}$ $T_{S}^{IN}$ $T_{S}^{IN}$ $T_{S}^{IN}$ $T_{w}$ $t$ $t$ $t$	reaction <i>j</i> Reaction rate at the surface of the particle, <i>A</i> , <i>B</i> , <i>C</i> Reaction rate at location <i>x</i> Distance from the particle centre Reactor radius Particle radius Ideal gas constant Reynolds number of liquid Reynolds number of gas Surface shape factor Schmidt number of liquid Sherwood number Temperature Temperature of the fluid Initial temperature of the fluid Initial temperature of the solid Initial temperature of the solid Temperature of the wall Time Fluid velocity	[mol/(g s)] [mol/(g s)] [] [m] [m] [m] [J/(mol K)] [] [] [] [] [K] [K] [K] [K] [K] [K] [K
$r_{i,S}$ $r_{i,x}$ $r_p$ $R$ $R_p$ $R_g$ $Re_L$ $Re_G$ $S$ $Sc_L$ $Sh$ $T$ $T_F$ $T_F^{IN}$ $T_S$ $T_S^{IN}$ $T_S$ $T_S^{IN}$ $T_w$ $t$ $t$ $t$	reaction <i>j</i> Reaction rate at the surface of the particle, <i>A</i> , <i>B</i> , <i>C</i> Reaction rate at location <i>x</i> Distance from the particle centre Reactor radius Particle radius Ideal gas constant Reynolds number of liquid Reynolds number of gas Surface shape factor Schmidt number of liquid Sherwood number Temperature Temperature of the fluid Initial temperature of the fluid Initial temperature of the solid Initial temperature of the solid Temperature of the wall Time Fluid velocity Stoichiometric coefficient of	[mol/(g s)] [mol/(g s)] [] [m] [m] [m] [J/(mol K)] [] [] [] [] [K] [K] [K] [K] [K] [K] [K
$r_{i,S}$ $r_{i,x}$ $r_{p}$ $R$ $R$ $R_{p}$ $R_{g}$ $Re_{L}$ $Re_{G}$ $S$ $Sc_{L}$ $Sh$ $T$ $T_{F}$ $T_{S}^{IN}$ $T_{S}^{IN}$ $T_{S}^{IN}$ $T_{w}$ $t$ $t$ $u_{F}$ $v_{A}$	reaction <i>j</i> Reaction rate at the surface of the particle, <i>A</i> , <i>B</i> , <i>C</i> Reaction rate at location <i>x</i> Distance from the particle centre Reactor radius Particle radius Ideal gas constant Reynolds number of liquid Reynolds number of gas Surface shape factor Schmidt number of liquid Sherwood number Temperature Temperature of the fluid Initial temperature of the fluid Initial temperature of the solid Initial temperature of the solid Temperature of the wall Time Fluid velocity Stoichiometric coefficient of component <i>A</i>	[mol/(g s)] [mol/(g s)] [] [m] [m] [m] [J/(mol K)] [] [] [] [] [K] [K] [K] [K] [K] [K] [K
$r_{i,S}$ $r_{i,x}$ $r_{p}$ $R$ $R$ $R_{P}$ $R_{g}$ $Re_{L}$ $Re_{G}$ $S$ $Sc_{L}$ $Sh$ $T$ $T_{F}$ $T_{F}^{IN}$ $T_{S}^{IN}$ $T_{S}^{IN}$ $T_{w}$ $t$ $u_{F}$ $v_{A}$ $V_{L}$ , $V_{G}$	reaction <i>j</i> Reaction rate at the surface of the particle, <i>A</i> , <i>B</i> , <i>C</i> Reaction rate at location <i>x</i> Distance from the particle centre Reactor radius Particle radius Ideal gas constant Reynolds number of liquid Reynolds number of gas Surface shape factor Schmidt number of liquid Sherwood number Temperature Temperature of the fluid Initial temperature of the fluid Initial temperature of the solid Initial temperature of the solid Initial temperature of the wall Time Fluid velocity Stoichiometric coefficient of component <i>A</i> Molar volume of component <i>A</i> and <i>B</i>	[mol/(g s)] [mol/(g s)] [] [m] [m] [m] [J/(mol K)] [] [] [] [[] [K] [K] [K] [K] [K] [K] [
$r_{i,S}$ $r_{i,x}$ $r_{p}$ $R$ $R$ $R_{p}$ $R_{g}$ $Re_{L}$ $Re_{G}$ $S$ $Sc_{L}$ $Sh$ $T$ $T_{F}$ $T_{S}^{IN}$ $T_{S}^{IN}$ $T_{S}^{IN}$ $T_{w}$ $t$ $u_{F}$ $v_{A}$	reaction <i>j</i> Reaction rate at the surface of the particle, <i>A</i> , <i>B</i> , <i>C</i> Reaction rate at location <i>x</i> Distance from the particle centre Reactor radius Particle radius Ideal gas constant Reynolds number of liquid Reynolds number of gas Surface shape factor Schmidt number of liquid Sherwood number Temperature Temperature of the fluid Initial temperature of the fluid Initial temperature of the solid Initial temperature of the solid Sherwood number Temperature of the solid Initial temperature of the solid Initial temperature of the solid Tomperature of the wall Time Fluid velocity Stoichiometric coefficient of Component <i>A</i> Molar volume of component <i>A</i> and <i>B</i> Volumetric flowrate of liquid and gas	[mol/(g s)] [mol/(g s)] [] [m] [m] [m] [J/(mol K)] [] [] [] [] [K] [K] [K] [K] [K] [K] [K
$r_{i,S}$ $r_{i,x}$ $r_{p}$ $R$ $R$ $R_{P}$ $R_{g}$ $Re_{L}$ $Re_{G}$ $S$ $Sc_{L}$ $Sh$ $T$ $T_{F}$ $T_{F}^{IN}$ $T_{S}^{IN}$ $T_{S}^{IN}$ $T_{w}$ $t$ $u_{F}$ $v_{A}$ $V_{L}$ , $V_{G}$	reaction <i>j</i> Reaction rate at the surface of the particle, <i>A</i> , <i>B</i> , <i>C</i> Reaction rate at location <i>x</i> Distance from the particle centre Reactor radius Particle radius Ideal gas constant Reynolds number of liquid Reynolds number of gas Surface shape factor Schmidt number of liquid Sherwood number Temperature Temperature of the fluid Initial temperature of the fluid Initial temperature of the solid Initial temperature of the wall Time Fluid velocity Stoichiometric coefficient of component <i>A</i> Molar volume of component <i>A</i> and <i>B</i> Volumetric flowrate of liquid and gas Volume of the particle and volume	[mol/(g s)] [mol/(g s)] [] [m] [m] [m] [J/(mol K)] [] [] [] [] [K] [K] [K] [K] [K] [K] [K
$r_{i,s}$ $r_{i,x}$ $r_{p}$ $R$ $R$ $R_{p}$ $R_{g}$ $Re_{L}$ $Re_{G}$ $s$ $Sc_{L}$ $Sh$ $T$ $T_{F}$ $T_{F}^{IN}$ $T_{S}$ $T_{S}^{IN}$ $T_{w}$ $t$ $u_{F}$ $v_{A}$ $V_{L}$ , $V_{G}$ $V_{p}$ , $V_{x}$	reaction <i>j</i> Reaction rate at the surface of the particle, <i>A</i> , <i>B</i> , <i>C</i> Reaction rate at location <i>x</i> Distance from the particle centre Reactor radius Particle radius Ideal gas constant Reynolds number of liquid Reynolds number of gas Surface shape factor Schmidt number of liquid Sherwood number Temperature Temperature of the fluid Initial temperature of the fluid Initial temperature of the solid Initial temperature of the solid Temperature of the wall Time Fluid velocity Stoichiometric coefficient of component <i>A</i> Molar volume of component <i>A</i> and <i>B</i> Volumetric flowrate of liquid and gas Volume of the particle and volume element <i>x</i>	[mol/(g s)] [mol/(g s)] [] [m] [m] [m] [J/(mol K)] [] [] [] [] [K] [K] [K] [K] [K] [K] [K

	Companii ai al li avoi de collegitore	[ /-]
$w_L$	Superficial liquid velocity	[m/s]
$We_L$	Weber number for liquid	
$x_A$ , $x_B$	Mole fractions of component A and	[]
	solvent	r 1
$x_i$	Volume fraction	
$X_G$	Lockhardt-Martinelli ratio	
<i>z</i>	Axial location	[m]
$\beta_{nc}$	Non capillary liquid hold-up	
$\Delta H_{ads,i}$	Adsorption energies for component $i$ ,	[J/mol]
ATT	i = A, B, C	[T / 1]
$-\Delta H_r$	Reaction enthalpy	[J/mol]
$dp/dz$ , $\Delta p/\Delta z$	Pressure gradient	[Pa/m]
$lpha_i$	Exponent for component <i>i</i>	[]
α	Parameter	
α	Maximum coverage	
α	Thermodynamic correction factor for	[]
2	diffusivity in liquid	r 1
β	Parameter	
$oldsymbol{eta}_i$	Exponent for component i	
$\gamma_I$	Exponent for component k	
$oldsymbol{\delta}_i$	Exponent for component <i>l</i>	[]
$arepsilon_L$	Liquid hold-up	
$arepsilon_F$	Fluid void fraction	
$\boldsymbol{arepsilon}_{B}$	Porosity of the catalyst bed	
$oldsymbol{arepsilon}_{P}$	Particle porosity	
$\eta_{e,i}$	Effectiveness factor of component <i>i</i>	
$\lambda_S$ , $\lambda_B$ , $\lambda_p$ , $\lambda_F$ , $\lambda_L$	Conductivity of solid, bed, particles, fluid, and liquid	[W/(m K)]
$\lambda_{z,F}$	Axial heat conductivity	[W/(m K)]
$\lambda_{r,F}$	Radial heat conductivity	[W/(m K)]
$\mu_L$ , $\mu_G$ , $\mu_M$ , $\mu_i$	Liquid, gas and mixture and component <i>i</i> viscosities	[kg/(m s)]
$\mu_B$	Viscosity of solvent	[cP]
ν	Kinematic viscosity	$[m^2/s]$
$ ho_L$ , $ ho_G$ , $ ho_B$ , $ ho_F$	Density of liquid, gas, particles and	[kg/m <sup>3</sup> ]
7277 677 8771	fluid	. 0.
$\rho_{cat}$	Catalyst mass concentration	$[kg_{cat}/m^3]$
σ	Surface tension	[N/m]
$\cup_{i,j}$	Stoichiometric coefficient for	[]
-1)	component <i>i</i> in phase <i>j</i>	
$\phi_L$	Dynamic liquid fraction	[]
$\phi$	Dissociation factor	[]
$\psi_L$ , $\psi_G$	Ergun equation left hand sides for	
	gas and liquid phases	

# 1 Background

Heterogeneous catalysis is one of the key technologies of our modern, highly industrialized society. Solid heterogeneous catalysts enhance the rates of chemical reactions without being consumed in them. This very fundamental definition, which dates back to the famous Swedish chemist Jöns Jacob Berzelius (1835), is still valid. The development of solid catalysts, such as iron-based catalysts for ammonia synthesis, nickel and noble metal catalysts for hydrogenation, cobalt-molybdenium catalysts for hydrode-sulphurization and hydrodeoxygenation and zeolite catalysts for hydrocarbon transformation, has guaranteed us a continuous and increasing delivery of fertilizers and fuel components, it has enabled a high standard of living for millions of people and it has also enabled the enormous growth of the human population, with all its advantages and disadvantages. Besides the production of bulk components, heterogeneous catalysis plays an enormous role in the preparation of fine and specialty chemicals, as well as pharmaceuticals and alimentary products. Drugs, perfumes, sweeteners, herbicides and pesticides are produced with the aid of heterogeneous catalysts.

The chemical applications are wide, but from the viewpoint of chemistry, physics and chemical engineering, all the man-made catalytic processes have similar features. It is usually claimed that more than 90 % of the industrially applied chemical processes are based on the use of catalysts, but 100 % of them take place in chemical reactors, i.e. in equipment particularly designed to carry out the catalytic transformation in a best

possible way, so that a high productivity and product selectivity is achieved. Good productivity combined with high selectivity is the primary goal for any catalyst development. These two targets are hard to achieve simultaneously for most applications and, therefore, an enormous amount of experimental effort is demanded worldwide, in academia and in industry. As a reward of the collective effort, catalysts have managed to revolutionize individual chemical production processes. High selectivity often implies a simpler process concept and, consequently, lower investment and operating costs. In most cases, however, chemical industry has to cope with multi-component feedstock and, in addition, by-product formation is often inevitable. Therefore, complicated separation steps are often required for final recovery of a desired main product and valuable by-products.

Many of the chemical applications of heterogeneous catalysis comprise three-phase systems, in which a gas and a liquid phase interact with a solid catalyst. Typical examples are catalytic hydrogenation, hydrodesul-phurization and hydrodeoxygenation processes, in which gaseous hydrogen react with an organic phase. A multitude of reactor constructions are available for continuous, heterogeneously catalyzed gas-liquid reactors. All these reactors have to satisfy the following two demands. First, the gas has to be brought into a very good contact with the liquid to minimize the gas-liquid mass transfer resistance. Secondly, liquid has to be brought into a good contact with the catalyst, since the reaction takes place only when the dissolved reactants in the liquid bulk phase reach the active sites on the catalyst surface. The workhorse for catalytic three-phase processes is a fixed bed reactor, in which the solid catalyst exists either in form of particles or fixed structures, such as structured elements or monoliths. Fixed bed reactors try to meet the respective demands by having the liquid flow on particle surfaces, thus providing a large surface area for mass transfer to occur, or by using porous catalysts, the pores of which are filled with the liquid by capillary forces.

Continuous fixed bed reactors are practical for long duration catalyst screening because they do not demand frequent filling and emptying as batch and semi-batch reactors do. Fixed beds are especially well suited for studying how well the solid catalyst keeps its long-term activity over the time. If a parallel set of multiple continuous reactors is used, operating in such a way that each reactor is either under different process conditions (pressure, temperature, liquid and gas flows) or loaded with different catalysts, a large amount of experimental data can be generated simultaneously, although the sampling has yet to be taken sequentially. Fixed bed reactors are also used in order to eliminate the possible losses of catalyst.

### 2 Reactor set- up

A fixed bed reactor system designed by us for catalyst and flow screening as well as kinetic studies is displayed in Figure 1. Several tubular reactors are placed in parallel in an oven to guarantee a homogeneous background temperature and to keep the fluidity of the liquid-phase components high enough for feeding. Each reactor is heated separately by a heating element, which implies that several reaction temperatures can be screened simultaneously. The gas and liquid feeds are controlled by mass flow controllers and HPLC pumps, respectively. In this way, the gas and liquid feeds can be altered independently. Catalyst particles or structured elements are placed in the reactor tubes. Typically, the catalyst is diluted with inert material to keep the individual reactor as isothermal as possible. The temperature in the bed is measured by thermocouples. Pressure and temperature data are stored on a computer. Gas and liquid-phase samples are analyzed on-line or off-line, depending on the chemical case. The equipment is particularly suitable for the investigation of catalytic two and three-phase systems, but it can be used for non-catalytic applications, too. The solid catalyst can be efficiently pretreated before its use; for instance, a hydrogenation catalyst can be reduced without any contamination at elevated temperatures under hydrogen flow before switching the reactant flow on. By varying the flow rates, the effect of the liquid and gas residence times is screened and the time-on-stream behaviors of the outlet concentrations reveal the catalyst stability. The role of internal diffusion in the catalyst particles is investigated by placing particles of different sizes in the parallel reactor tubes. Because the chemical analysis is the bottle-neck in the parallel screening of catalysts, it does not make sense to couple too many reactors in the system; in any case, offline analysis becomes the limiting step in the research project. Therefore, instead of high throughput screening, we call the concept reasonable throughput screening.

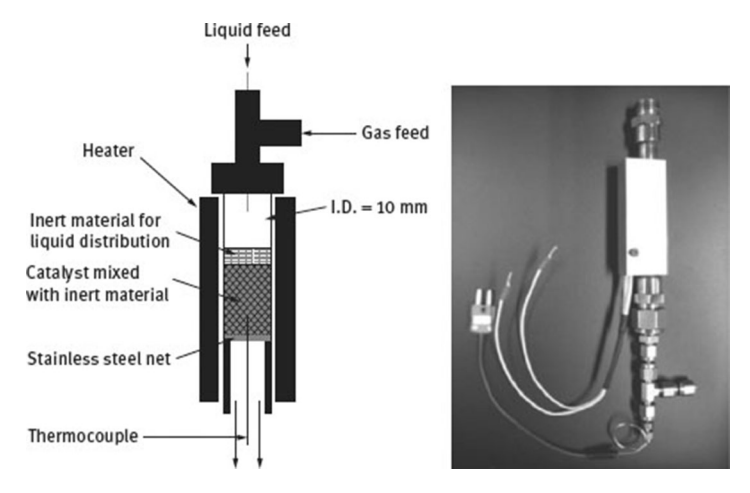


**Figure 1:** Parallel reactor set-up for reasonable throughput screening in laboratory scale [46]. Reprinted with permission from Ind. Eng. Chem. Res., 2012, 51 (26), pp 8858–8866.

## 3 Physical and chemical phenomena in fixed bed reactors

### 3.1 Overview

The major issues concerned in fixed bed studies are summarized in Figure 2. Fixed bed reactors operating under the trickling flow regime are among the most commonly selected continuous reactor alternatives and are, therefore, the focal point of interest in both experimental and modeling studies. With the experience presented in open literature [1–8], the modeling of three-phase fixed bed reactors still remains challenging for every new reaction system, because the extent and the importance of each individual effect is very case-specific and strongly dependent on actual operating conditions (temperature, pressure, liquid and gas flow rates and feed concentrations), physical properties of gases and liquids in question and the properties of the catalyst (activity, particle size and shape, porosity, pore structure, metal loading, metal dispersion, oxidation state).

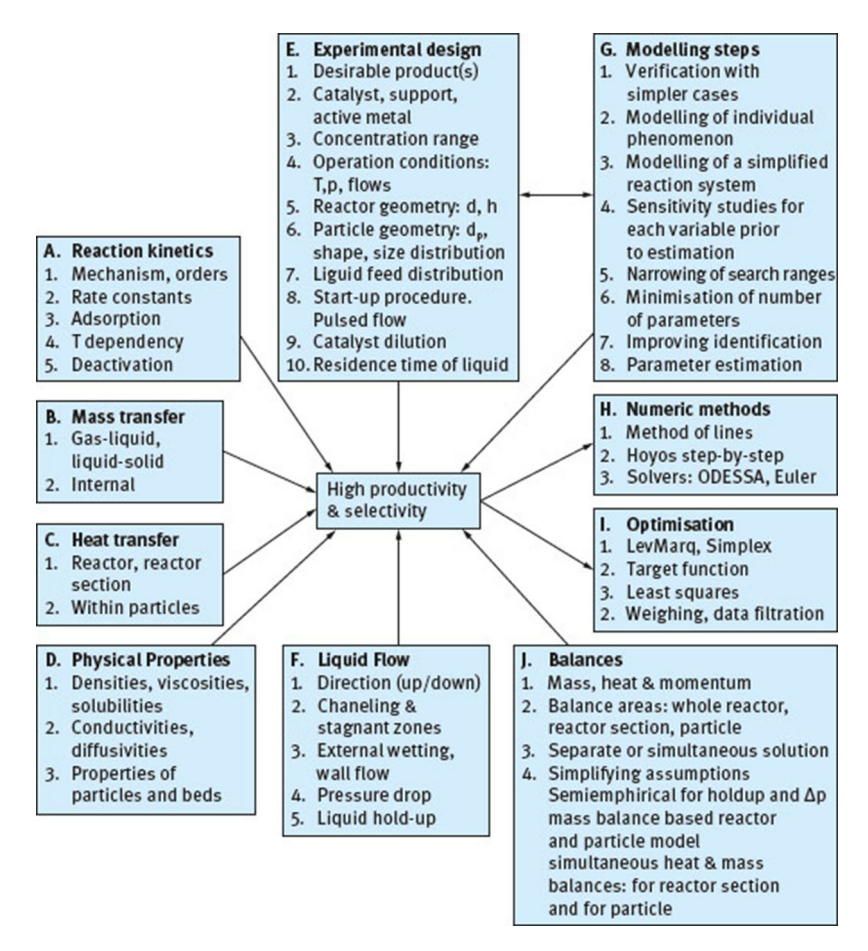


Figure 2: Major issues of continuous fixed bed reactor studies [9].

Figure 2 summarizes the key issues to be faced and the means to cope with these challenges in the experimental and modeling studies of continuous fixed bed reactors operating at the trickling flow regime. Just a glance at this overview of topics gives an immediate reminder that these kinds of reactors are surprisingly complicated systems, both to study experimentally and especially to model mathematically, although they initially might look like simple ones (just a pipe filled with particles and flows). The complicated nature arises from the facts that three phases are always involved, that multiple reactions proceed simultaneously and that the particles of various sizes typically have irregular shapes in a laboratory scale. Although three-phase systems are so commonly used in the chemical industry, they are among the most challenging ones to be modeled. Complicated geometry is also well known to add further challenges especially for detailed description of fluid dynamics. This implies that several simplifications are required to progress with the modeling effort of a continuous fixed bed reactor operating in the trickling flow regime.

## 4 Research targets and topics

### 4.1 Catalyst selection

High productivity and selectivity are the obvious goals for reaction engineering and reactor design. The intrinsic kinetics are strongly dependent on the catalyst used. Thus, the catalyst selection and preparation both play a vital role in the success of all the conducted studies. The catalysts used in laboratory-scale reactors are either tailor-made or commercial ones. The key issues in the operation and modeling of fixed beds for three-phase processes are summarized below.

### 4.2 Reaction kinetics

Temperature and concentration-dependent multiple reaction kinetics determine largely both the productivity and selectivity (if the system is not under mass transfer control). Therefore, modeling of the reaction kinetics

is an essential part of all our studies. Each reactant must reach and adsorb the active sites of the catalyst to react there. This may limit the reaction rates, especially, when dealing with concentrated solutions. Therefore, also the adsorption kinetics are to be considered in the modeling study. Deactivation is a phenomenon to be expected in long-term continuous operation sooner or later.

### 4.3 Mass transfer effects

The required steps of mass transfer (from gas to liquid phase, from liquid to solid surface and finally internal diffusion) can limit both productivity and selectivity, the more so, the faster the intrinsic reaction rates are.

### 4.4 Heat effects

Whenever exothermic reactions produce too much heat to be effectively transferred away, temperature gradients emerge. The most severe ones typically are radial temperature gradients inside the reactor and within individual particles (in normal cases where the axial temperature is tried to be kept constant by means of a cooling jacket).

### 4.5 Physical properties of gases and liquids

Physical properties of the solutions determine not only how well the fluids flow and how much liquid is retained in the fixed bed, but also how well mass and heat are transferred. By a proper selection of the operation conditions and catalyst/support properties, the physical properties can be adjusted to be more favorable; in that way, the reactor performance can be enhanced.

### 4.6 Reactor design and operation policy

The details of the reactor design (particle sizes and shapes, feed distribution, start-up procedure, catalyst loading, bed dilution) all play an essential role in determining how ideal flow fields (without channeling and wall flow) are generated and how effectively the reactor is used. One can suppress and minimize the effects of undesirable heat and mass transfer as well as flow related phenomena by proper selections of reactor design and operation conditions. Mathematical modeling in many cases works hand in hand with experimental design. On the one hand, it sets demands for the experimental work and, on the other hand, it tries to extract a maximum amount of know-how from experiments conducted to figure out and explain what really took place in the reactor. A very essential part of the experimental design is to generate ideas on how the interrelated phenomena could be separated from each other and how an extensive modeling task can be divided into multiple smaller sub-tasks.

Gravity driven down-flow of a liquid was used in all our cases. The formation of ideal flow fields of liquid was, on the one hand, aimed at by using a fine sand bed feed distributor; on the other hand, by diluting the catalyst with small inert particles.

### 4.7 Modeling options

The solutions of the modeling tasks are strongly based on the application of numerical mathematical methods and in most cases demand case-specific parameter optimizations.

Many of the models for individual phenomena are to be fine-tuned by parameter adjustment. Efficient algorithms for the minimization of the least square differences between observations and predictions are widely used. Data filtration is used whenever experimental points are clearly out of the pattern. Weighing is in some cases applied to improve the model accuracy in the vicinity of the most interesting results (results providing the highest productivities and selectivities).

The models have their origins in the conservation laws of nature: mass, energy and momentum balances. Momentum balances are often systematically replaced by semi-empirical expressions, and the liquid flow is described by a simple interpretation of results by using an axial dispersion model for backmixing and semi-empirical equations for liquid hold-up and pressure drop. In many isothermal cases, mass balances and semi-empirical expressions together with kinetic expressions (including catalyst deactivation) can be used to describe

the reaction system in a satisfactory manner. A simultaneous solution of dynamic and steady state mass and heat transfer models is demanded when heat generation via reactions is considerable.

## 5 Experimental design

Experimental design is a crucially important issue for the success of a research project devoted to catalytic three-phase systems. The main features of experimental design are summarized in Figure 3.

Experimental design		
A. Desirable targets     a) Directly value adding materials.     b) Platform chemicals.     c) Simplified production processes.	<ul> <li>F. Particle geometry</li> <li>a) The smaller, the less serious T and C gradients.</li> <li>b) Smaller particles evens flow. c) higer Δp.</li> <li>c) Large surface shape factor desirable.</li> </ul>	
B. Catalyst selection     a) Based on activity and selectivity.     b) Candidates mentioned in literature.     c) Expertise in our laboratory.	G. Feed distribution a) To establish fine flow patterns. b) Fine sand bed an example.	
C. Concentration range a) Dilute: Eliminates undesired T and C gradients. Well suited for catalyst screening studies. b) Concentrated: Favored by industry. Exception: Recovery from waste streams.	H. Start-up procedure     a) Flow patterns remain to stay.     b) Pulsing feed flow leads to higher productivity.     c) Initial flooding recommended.	
D. Operation conditions p,T a) Temperature influences often selectivity. Max. temperature giving good selectivity. b) Pressure improves gas solubility.	Catalyst dilution     a) Less severe T and C gradients.     b) May improve flow patterns.     c) Danger: Catalyst by-passing.	
Diameter, height     a) (Particle diameter)/(Reactor diameter):     to eliminate chanelling and wall flow.     b) Height to offer reasonable conversion.	J. Residence time a) Long enough for reactions to occur. b) Distribution unavoidable.	

**Figure 3:** Key issues in experimental design [9].

### 5.1 Targeted products

Desirable targets are typically value-added product compounds (and/or) product compounds that lead the way to simplified production processes.

### 5.2 Catalyst screening

The goal is first to screen best candidates for catalyst/support and then to reveal how the productivity and selectivity can be further enhanced by optimizing the operating conditions. In catalyst screening, experience on systems of a similar nature helps considerably by limiting the number of potential candidates.

### 5.3 Experimental productivity and selectivity optimization

When making kinetic experiments in continuous fixed bed reactors, complete conversion is to be avoided in order to reveal the reaction kinetics. The operation conditions, T, p,  $u_L$ , and  $u_G$  can be selected according to the following reasoning. Typically, the temperature rise accelerates reaction rates exponentially. When reaching an acceptable productivity, the selectivity becomes the major issue according to which the operation temperature is to be optimally selected. The reason why the selectivity of a desirable product compound is often temperature dependent is that activation energies for various reactions are different. The generation of undesirable side products is to be avoided, because they may demand additional separation steps in down-stream processing. In order to have a high gas solubility, high partial pressure of the gaseous component is required. In shallow laboratory reactors, the liquid flow is adjusted to low in order to provide reactions enough residence time to progress in detectable extents. Gas is often fed in excess. Diluted streams are often used to reduce the undesirable mass and heat transfer effects.

### 5.4 Particle geometry

In our catalyst screening tests, typically, the reactor diameter was around 1 cm or less and the reactor length was case dependent. Small catalyst particles were used to generate better flow fields and to provide a higher specific surface area without generating an unacceptably high drop in pressure within the short laboratory reactors. In our studies, the catalyst particles were sieve fractions of crushed particles. The second largest dimension was their characteristic mean size. The external surface area of a particle is well known to be proportional to the  $2^{\rm nd}$  and the volume to the  $3^{\rm rd}$  power of characteristic size, thus making the smallest and the largest particles of a sieve fraction very different. Mass transfer limitations normally become the most severe within the largest particles. Krisher-Kast hydraulic diameter ( $d_K$ ) is frequently used as the characteristic particle size for packed beds, because it accounts for the bed porosity effect [10]. Mean sizes were calculated straight from the largest and the smallest sizes, when the particle size distribution was not available. If the particle size distribution were known, it could have been included in the reactor model [11]. The geometry of randomly packed trickle bed reactors is very complicated, especially when the catalyst bed consists of particles having a distribution of sizes and even more so when particle shapes are irregular. In CFD studies, the detailed fixed bed geometry can be taken into account only for more regular particle shapes.

### 5.5 Feed distribution and flow regimes

The liquid feed is targeted to be well distributed. A simple yet effective feed distributor for small-scale operation is a fine sand bed. Complete external wetting of all catalyst particles is easier to get when liquid is initially well distributed.

Fixed bed reactors are commonly operated under the trickling flow regime. Under these conditions, the way the operation is started determines to a large extent how fine liquid flow fields are generated. Initial flooding of the bed or a short visit to the pulse flow regime *a priori* helps to reduce channeling and can do it, surprisingly, permanently [12]. The pulse flow regime can be a more effective operation mode than the trickling flow regime, since pulses continually even the mal-distribution of the flow. However, only higher superficial velocities of liquid and gas can generate pulsed flow. This shortens residence times, if a longer reactor is not used. The artificial generation of pulsed flow at lower flow rates has been studied simply by making feed flow variations [13]. There, high and low liquid holdup periods were forced to take their turns repeatedly with adjustable period lengths. However, the fluctuations in the liquid flow did not progress far inside the reactor. In pilot scale styrene hydrogenation, liquid feed fluctuation has been reported to give a higher yield.

### 5.6 Bed dilution

Temperature gradients can be lowered by diluting the catalyst bed with highly conductive inert particles. The generated heat per unit volume of the bed depends directly on the bed dilution. The more the catalyst bed is diluted, the more difficult it becomes to avoid catalyst bypassing. Small particles are especially well suited for dilution because they improve catalyst wetting [10].

### 5.7 Residence time distribution

Typically, any back-mixing decreases the productivity. Therefore, it is essential to include it in the reactor models. If dispersion takes place and is not included, this leads to an underestimation of the productivity (and erroneous values of kinetic parameters). The single parameter axial dispersion model is the standard way of taking into account the back-mixing effect and the consequent broadening of the liquid residence time distribution [3]. The axial dispersion model adds a second order spatial derivative term in the liquid mass balances. It works punctually in the two extreme cases (for the most productive mode of operation (plug flow), and the least productive mode (continuous ideal mixing of liquid)). The axial dispersion model is unable to predict a sometimes visible tail in the distribution caused by the presence of stagnant zones. For such cases, the piston flow exchange model is a more precise modeling option. It has two adjustable parameters. The liquid flow in this model is thought to consist of two streams (one flowing rapidly, the other flowing slowly) and mass exchange is modeled to take place in between these streams.

### 6 Chemical kinetics

### 6.1 Topics of the kinetic studies

The intrinsic rates of heterogeneously catalyzed reactions are described with chemical kinetics; this explains how the reaction rates depend on concentrations, temperature and the nature of catalyst. Chemical kinetics together with other means of studying catalytic reactions, such as spectroscopy of catalysts, molecular modeling and calculation of the thermodynamics of reactants, intermediates and products, form the basis for understanding chemical processes.

Experimental kinetic investigations are the basis of revealing reaction mechanisms. The following problems can be solved by using a kinetic model:

- choosing the catalyst and comparing the selectivity and activity of various catalysts and their performance under optimum conditions for each catalyst;
- the determination of the main and by-products formed during the process;
- the determination of the optimum sizes and structures of catalyst grains and the necessary amount of the catalyst to achieve the specified values of the selectivity of the product and conversion of the starting material;
- the determination of the short and long time stability of the catalyst;
- the determination of the stability of steady states and parametric sensitivity; that is, the influence of deviations
  of all parameters on the steady state regime and the behavior of the reactor under unsteady state conditions;
- the study of the dynamics of the process and decision if the process should be carried out under unsteady state conditions;
- the study of the influence of mass and heat transfer processes on the chemical reaction rates and product selectivities as well as the determination of the kinetic region of the process;
- selection of the type of a reactor and structure of the contact unit that provide the best approach to the optimum conditions.

The method which simplifies the kinetic treatment and reduces the number of parameters in the mathematical model is the quasi-steady state approximation (QSSA) originally developed by Bodenstein in 1913.

### 6.2 Reaction scheme simplifications

In general, a reaction is considered to be at steady state, if the concentrations of all species in each element of the reaction space (volume for a homogeneous reaction or surface for a heterogeneous reaction) do not change in time. In general, such conditions are fulfilled in open systems, such as continuous tank and tubular reactors and in flow circulation reactors. Grouping the reaction species in two categories – reaction intermediates in one, and reactants (substrates) and products in another one – it can be stated, for reaction participants at a steady state, that if a species enters an element of the reaction space, its concentration does not change with time, while for intermediates, the production rate is equal to the consumption rate. Bodenstein proposed that there are intermediates in chemical reactions that are present in "inferior" amounts, e.g. in much lower concentrations than the major species in the mechanism. If this condition is met, the rate of change of the concentration of the intermediate can be considered negligible. The application of the steady state approximation to heterogeneous catalysis does not require that the surface concentrations are low, but implies that they do not essentially change with time.

Another frequently used approximation in catalytic kinetics is the quasi-equilibrium approximation, which implies that one step in a multistep catalytic reaction sequence is much slower than the other ones. In such a case, the other steps can be considered as being close to the equilibrium, as their forward and backward rates will be close to each other. The quasi-equilibrium approach, utilized very often, limits the description of catalytic kinetics as it discards transient processes. It is, however, frequently used to obtain simplified and useful expressions for reaction rates. Typically the surface reaction rate is assumed to be rate-limiting, whereas the adsorption and desorption steps are presumed to be rapid. The approach should be supported by experimental evidence obtained by measurements of the reaction and adsorption rates. In the case of complex reactions, several steps are possible and a rigorous treatment is required comprising a multistep rate control, as the quasi-equilibrium approach cannot be applied.

### 6.3 Rate expressions

The rate equations depend heavily on the particular chemical case of interest. Typically, the process involves a reaction between a large organic molecule and a much smaller reagent molecule (e.g. oxygen or hydrogen). In this case, the overall rate is often controlled by the surface reaction step, whereas the adsorption and desorption steps are assumed to be rapid. Further assumptions are needed concerning the details of the reactant adsorption. Both competitive and non-competitive adsorption models have been proposed and used to describe the kinetics. A non-competitive adsorption model can be justified by the size difference of the reacting molecules. A general overview of kinetic models is provided by [4] and [14], where also a semi-competitive adsorption model is discussed. It has been successfully applied to sugar hydrogenation [15].

Some generalization of classical kinetic models is possible. For a bimolecular and reversible reaction A + B = C + D, the rate takes the form of (Eq. 1).

$$R = \frac{\text{kinetic factor} \cdot \text{driving force}}{(\text{adsorption term})^n}$$
 (1)

where the adsorption term includes  $K_AC_A$ , etc. for molecular adsorption or  $(K_AC_A)^{1/2}$  for dissociative adsorption, and the power in denominator corresponds to the number of species in the rate determining steps, while the driving force is  $(1 - C_CC_D)/(K_{eq}C_AC_B)$ . The adsorption of molecules can be of a competitive nature, but in cases when the molecules represent very different sizes, such as catalytic hydrogenation of organic components, non-competitive adsorption is assumed. A rather general rate equation comprising the rate limitation by the surface reaction step as well as both competitive and non-competitive adsorption can be written as (Eq. 2):

$$r_{j} = \frac{k_{j} \left( \prod C_{i}^{\alpha i} - C_{i}^{\beta i} / K_{j} \right)}{\left( \sum K_{k} C_{k}^{\gamma k} + 1 \right)^{m} \left( \sum K_{l} C_{l}^{\delta l} + 1 \right)^{n}} \tag{2}$$

For competitive adsorption, either m = 0 or n = 0. Of course, rate equations of this kind should be derived case by case, starting from a plausible mechanism.

Models with semi-competitive adsorption have been applied in the hydrogenation of aromatics and sugar molecules [16]. The principle of semi-competitive adsorption is that the large organic molecules always leave some empty space, i.e. vacant interstitial sites, where the smaller molecule (typically hydrogen and oxygen) can adsorb. Compared to the classical model, the semi-competitive adsorption model includes one additional parameter, namely the maximum coverage of the organic molecule [15].

The concept of semi-competitive adsorption of a large molecule and a smaller one implies that the maximum coverage of the large molecule is less than one, and thus some interstitial sites always remain accessible for the smaller molecule (such as hydrogen). For example, for irreversible catalytic hydrogenation of a large organic molecule (*A*) with molecular hydrogen (*H*), the following rate equation can be derived for the rate control of the surface reaction, (Eq. 3):

$$r = \frac{kK_A K_H C_A C_H \alpha ((1 - \alpha) K_A C_A + 1)}{((1 - \alpha) K_A K_H C_A C_H + K_A C_A + K_H C_H + 1)^2},$$
(3)

where  $\alpha$  is the maximum coverage of A (< 1). For the limit case  $\alpha$  = 1 and the standard Langmuir-Hinshelwood model is obtained from (Eq. 3). Generalizations of this concept are presented in literature [15, 16]. For highly non-ideal systems, activities should be used in the rate equations instead of concentrations.

### 6.4 Qualitative reaction rate comparison: fixed bed against batch reactors

Theoretically, the modeling of an ideal plug flow reactor and an ideally mixed batch reactor is almost identical. Similar mass balance equations can be used. The reaction time in the batch reactor corresponds to the space/time in the plug flow reactor. According to this analogy, the space/time represents a measure of how far the observation point has moved following the flow. The situation demands adaptations when focusing on multiphase flow in trickle beds. Liquid flow occupies only a part of the pipe volume and this is typically accounted for by introducing the liquid hold-up in the mass balances. The analogy still holds well if gas is abundantly available to saturate the liquid. In theory, the intrinsic kinetics on the active metal sites of the catalyst is exactly the same for both reactors, when exactly the same catalyst is used. The questions are whether all the reactants

can reach the active sites and how active the sites are. Uneven liquid flow (resulting from too low liquid velocity, too large particles or complex detailed geometry) is the key reason behind the deviations between the reaction rates of trickle bed and batch reactors. Low flow velocities may allow mass transfer resistances to arise and can also cause more severe local deactivation. In a fixed bed reactor, deactivation is location-dependent and often it is at its strongest close to the feed inlets where the concentration is on top. The catalyst deactivation in a batch reactor is much more uniform since all fluid elements face similar conditions. The main reasons discussed for deviations are summarized in Figure 4.



Figure 4: Reasons for kinetic deviations between a fixed bed reactor and a slurry reactor [9].

### 6.5 Catalyst deactivation

Sooner or later, the deactivation of a heterogeneous catalyst takes place. Generally, there are multiple reasons for it, but in our cases, the most probable reason was coking of organic reactant, which is well known to take place at elevated temperatures. Coke simply blocks pores and reactants cannot reach the active sites. Typically, the concentration curves show that after being initially fast, later on, the deactivation slows down and often finally becomes hardly detectable. Then it can be modeled using the concept of final activity. An analytical expression, (Eq. 4) is valid for first order power law kinetics. For cases following the Langmuir-Hinshelwood-Hougen-Watson kinetics, a numerical solution is the only alternative, since coking can then only be expressed with ordinary differential equations [9]. The equations are solved together with the dynamic mass balances. A couple of equations, Eqs. (4) and (5), for the catalyst activity (a), are listed below.

Analytical expression:

$$a = a_f + (a_0 - a_f) \exp(-k_d t) \tag{4}$$

Reactant concentration dependent deactivation:

$$-\frac{da}{dt} = \frac{(a - a_f) k_d C_{A,L}}{(1 + K_A C_{A,L} + K_B C_{B,L})}$$
(5)

In practice, the reaction rate equations are corrected for the catalyst deactivation by multiplying them with the activity factor (a). The deactivation rate parameter ( $k_d$ ) is temperature-dependent.

### 6.6 Truly intrinsic kinetics

Highly intensive mixing and very small catalyst particles are to be used to reveal truly intrinsic kinetics. An isothermal semi-batch slurry reactor, equipped with an adjustable stirrer speed, is an exceptionally well-suited device for that purpose. From these results, the truly intrinsic activation energies can also be obtained. Otherwise, various kinds of mass transfer resistances (gas-liquid, liquid-solid or internal) may be rate-limiting. Intrinsic kinetic rate constants depend typically far stronger on temperature than mass transfer coefficients. Therefore, in cases where the reported activation energies are low, it is possible that some of the mass transfer steps may be rate-limiting [4]. Since in many published reaction rate studies it is not absolutely clear, whether or not the kinetics were truly intrinsic, the safe option is to take only the forms of the kinetic expressions from literature.

### 7 Mass and heat transfer effects

### 7.1 Mass transfer resistances

In Figure 5, the mass transfer effects present in a three-phase system are qualitatively illustrated. The figure shows how the reactant concentration decreases due to mass transfer resistances along the way from bulk gas down to the active sites within a porous catalyst particle. In order to react, a gas-phase compound has to go all the way from the gas to liquid, from liquid to solid and finally penetrate inside the porous solid until it reaches the active site. Gas-liquid and liquid-solid mass transfer is typically expressed by power laws of dimensionless numbers. The steady state internal diffusion is described by an ODE.

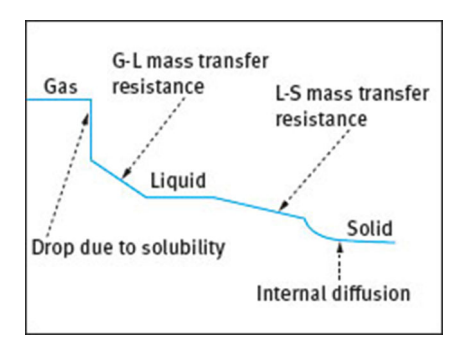


Figure 5: Mass transfer steps in a three-phase fixed bed reactor [9].

### 7.2 Gas-liquid mass transfer

For rapid reactions, gas-liquid mass transfer may become rate-limiting if mixing is not intensive. This can happen especially when the partial pressure of the limiting gas reactant is low. Then an increase in operating pressure may help, because it directly increases the solubility and thus the mass flux. Another way to increase the partial pressure of the rate-limiting gas reactant is to increase its mass fraction in the gas feed. This cannot always be done freely, since the explosive range may set limits to the maximum gas contents. Direct synthesis of hydrogen peroxide serves as an example of this kind of behavior.

Gas-liquid mass transfer restrictions can be overcome by providing a large interfacial mass transfer area and by using high superficial velocities to enhance the mass transfer. The liquid flows as a film on the surfaces of the particles and, therefore, the mass transfer area depends strongly on particle sizes, shapes and roughness of the external surfaces. For providing a reasonable residence time, the higher the superficial liquid velocity is, the longer the required reactor should be. Another way to increase liquid flow is to use liquid circulation. It suits best for a low yield system, the productivity of which is less sensitive to back-mixing.

When using gas-liquid mass transfer expressions from literature [10], in the range of very low superficial velocities, the equations give very different values [19, 20]. Most of the given mass transfer correlations are power laws of dimensionless numbers. Each dimensionless number represents either a geometric or a kind of force ratio. General agreement concerning which dimensionless numbers to include is still lacking. Differences can also clearly be seen in the values of gas and liquid flow exponents. If studies cover only a narrow temperature range, the physical properties can be treated as constants. Then superficial gas and liquid velocities become the only variables on which the mass transfer coefficients depend. Gas-liquid mass transfer does not easily become a limiting factor for dilute systems when the intrinsic reaction rates are low.

Mass transfer coefficient correlations are given in a review [10]. One typical gasliquid mass transfer correlation especially for the low interaction regime is given in (Eq. 6). The united gas-liquid mass transfer coefficient is expressed as a function of various dimensionless numbers, characteristic particle dimension and molecular diffusivity. The example equation is given in the following form:

$$\frac{k_l a d_K^2}{D_{A,L}} = 2.8 \cdot 10^{-4} \left( X_G^{1/4} R e_L^{1/5} W e_L^{1/5} S c_L^{1/2} G e o^{1/4} \right)^{3.4}$$
 (6)

$$X_G = \frac{w_G \sqrt{\rho_G}}{w_L \sqrt{\rho_L}} \tag{7}$$

── Kilpiö et al. DE GRUYTER

$$Re_L = \frac{\rho_L w_L d_p}{\mu_L} \tag{8}$$

$$We_L = \frac{\rho_L w_L^2 d_p}{\sigma} \tag{9}$$

$$Sc_L = \frac{\mu_L}{\rho_L D_{A,L}} \tag{10}$$

$$Geo = \frac{a_v d_k}{1 - \varepsilon_B} \tag{11}$$

Lockhardt Martinelli ratio, Reynolds, Weber, and Schmidt numbers of liquid and finally a geometric ratio (representing the catalyst properties) are used to calculate the united mass transfer coefficient ( $k_la$ ), Eqs. (7)–(11). The gas-liquid mass transfer coefficient depends on the diffusivity of the compound in question.

Gas-liquid mass transfer rates for a reactive and a non-reactive system differ from each other [21]. For a reactive system, rates are higher than for a corresponding absorption system. The reason behind the difference is probably the presence of stagnant liquid zones. In the case of absorption, these zones become saturated with gas. The saturation does not take place in a reactive system so easily because the reaction consumes the dissolved gas reactant.

### 7.3 Liquid-solid mass and heat transfer

Liquid-solid mass transfer depends on local liquid velocities and, therefore, in a trickle bed, it may become restricting especially in the places where liquid flows slowly. Correlations for liquid-solid mass transfer coefficients are provided in literature. The general principle for the correlations currently available is that the liquid-solid mass transfer coefficient for the liquid film surrounding the solid catalyst particles depends on the Reynolds (Re) and Schmidt (Sc) numbers [4], Eqs. (12)–(15). From these dimensionless numbers, the Sherwood (Sh) number is calculated and the liquid-solid mass transfer coefficient (k) is obtained:

$$Sh = A + BRe_I^{\alpha} Sc_I^{\beta}, \tag{12}$$

$$Sh = \frac{k_L d_p}{D_{i,L}},\tag{13}$$

$$Re_L = \frac{\rho_L w_L d_p}{u_L},\tag{14}$$

$$Sc = \frac{v_L}{D_{i.L}}. (15)$$

In an analogous manner, the heat transfer coefficient (h) for the liquid film can be calculated; the Nusselt number (Nu) is obtained from the Reynolds (Re) number and the Prandtl number (Pr), Eqs. (16)–(19):

$$Nu = A + BRe^{\alpha} Pr^{\beta}, \tag{16}$$

$$Nu = \frac{h_L d_p}{\lambda_I},\tag{17}$$

$$Re = \frac{w_L d_p}{v_L} = \frac{w_L d_p \rho_L}{\mu_L},\tag{18}$$

$$Pr = \frac{c_{p,L}\mu_L}{\lambda_L}. (19)$$

Coefficient *A* corresponds to the situation of stagnant flow and has a value around 2. The other parameters are of empirical character, typically  $\alpha = 0.6 - 0.7$ ;  $\beta = \frac{1}{3}$ . Coefficient *B* is close to 1.

Liquid-solid mass and heat transfer can depend a lot also on the pre-wetting procedure. This supports the finding that, if by initial wetting, the extent of channeling can be decreased; the generated flow fields will also remain to stay.

### 7.4 Internal diffusion – pore diffusion

The reaction rates are at their highest close to the feed entrance when the liquid feed stream is saturated with the gas reactants. Especially there, the reactants may not be able to diffuse as fast as the reactions could consume them and internal diffusion may become rate-limiting.

Small particles can be used in laboratory-scale trickle beds, because there they do not generate a high pressure drop. In large-scale operation, the pressure drop is an operating cost to be minimized. The use of small particles cannot be afforded then, and under these circumstances the particle shape becomes the primary factor with which to increase the surface-to-volume ratio [5].

By having particles with a high surface area-to-volume ratio, the importance of internal mass transfer resistance can be reduced. According to open literature [1], the most common regular shapes are spheres, cubes, hollow cubes, cylinders, hollow cylinders, four holes cylinders, single rings, cross webs, grooved cylinders, Pall rings, Intalox saddles and Berl saddles. One surface-to-volume ratio comparison study is reported for particles originating from a cylindrical structure. Discs, cylindrical extrudates, quadrulopes, rings, hollow extrudates, wagon wheels and miniliths had the surface area-to-volume ratio in increasing order. The ratio for the miniliths went up to 20. Various catalyst suppliers have also special geometries that, compared to cylinders, provide a manifold external surface-to-volume ratio.

The length of the diffusion path is another factor that directly determines the severity of internal mass transfer resistance. Short diffusion paths are highly desirable. They can be obtained in two ways: by well-selected particle geometry or by locating the active sites close to the external surface of the particles. In order to determine the severity of the internal diffusion, the effective diffusivity needs to be known. The most common way to calculate its value is to start from molecular diffusivities in liquid and make a simple porosity and tortuosity correction [4, 7].

### 7.5 Effectiveness factors for particles

The aim of an internal diffusion and heat conduction study is to determine the effectiveness factor for each component. It is a direct measure that tells how well the active sites of a catalyst particle are in use [4, 6]. If the diffusion is rapid and provides reactants to active sites so that the surface concentrations prevail everywhere, effectiveness factor is 1. Effectiveness factors are calculated because they are directly comparable for different particle geometries while internal concentration profiles are not. The effectiveness factor is defined as:

$$\eta_{e,i} = \frac{\int_0^{V_p} r_{i,x} dV}{r_{i,S} V_p}.$$
 (20)

(Eq. 20) tells that the effectiveness factor is obtained by integrating the rate obtained from the concentration profiles in the porous catalyst particle.

# 8 Physical properties of gas mixtures and solutions

The operating conditions (T, p), and the composition determine the physical properties of gas and liquid mixtures. When studying new reaction systems (multi-component mixtures at specified process conditions), the odds are frequently in favor of not finding exact values directly from open literature.

### 8.1 Density and viscosity

The proper approaches are either to use extrapolation or to take values from a resembling mixture. For extrapolation and interpolation of highly nonlinear liquid viscosities, one can use the functions from Properties of Gases and Liquids [22]. For estimates of viscosity, at least at two temperatures are required. The viscosities of a resembling mixture can also be taken as a starting point of extrapolation. Resembling organic compounds are the ones that have nearly the same chain length and contain similar functional groups. Linear extrapolation and interpolation work well for liquid densities. The most reliable way is experimental determination of unknown densities and viscosities.

—— Kilpiö et al. DE GRUYTER

### 8.2 Diffusivity

In the review of [23], several correlation equations were proposed and compared for liquid-phase diffusivity. Most of the correlations are based on the original Stokes and Einstein equation, where for practical purposes the radius of the solute molecule can be replaced by the molar volume of the solute. The Wilke-Chang equation has been favorably compared to other expressions; it has become popular [24]. Diffusivity of a component is mainly dependent on the molecule size, temperature and solvent viscosity. Some common correlations are listed below (A = solute, B = solvent).

Wilke-Chang (Eq. 21):

$$D_{A,B}^{0}/\left(\mathrm{m}^{2}/\mathrm{s}\right) = \frac{1.2 \cdot 10^{-16} \cdot \left(\phi M_{B}/\left(\mathrm{kg/kmol}\right)\right)^{0.5} (T/K)}{\left(\mu_{B}/\mathrm{Pa}\,\mathrm{s}\right) \left(V_{A}/\left(\mathrm{m}^{3}/\mathrm{kmol}\right)\right)^{0.6}}.$$
(21)

Scheibel equation for organic solvents (Eq. 22):

$$D_{A,B}^{0}/\left(m^{2}/s\right) = \frac{8.2 \cdot 10^{-16} \left(T/K\right)}{\left(\mu_{B}/Pa \, s\right) \left(V_{A}/\left(m^{3}/kmol\right)\right)^{1/3}} \left(1 + \left(\frac{3\left(V_{B}/\left(m^{3}/kmol\right)\right)}{\left(V_{A}/\left(m^{3}/kmol\right)\right)}\right)^{2/3}\right). \tag{22}$$

Reddy and Doraiswamy equation for water as the solute in various solvents (Eq. 23):

$$D_{A,B}^{0}/\left(m^{2}/s\right) = \beta \frac{\left(T/K\right) \left(M_{B}/\left(kg/kmol\right)\right)^{0.5}}{\left(\mu_{B}/Pas\right) \left(\left(V_{A}/\left(m^{3}/kmol\right)\left(V_{B}/\left(m^{3}/kmol\right)\right)^{1/3}\right)},$$

$$\beta = 10 \cdot 10^{-17}, V_{B}/V_{A} < 1.5, \qquad \beta = 8.5 \cdot 10^{-17}, V_{B}/V_{A} \ge 1.5.$$
(23)

Fedors equation for viscous liquids, (Eq. 24):

$$D_{A,B}^{0} / (m^{2}/s) = 4.5 \cdot 10^{-15} \frac{(T/K)}{(\mu_{B}/\text{Pa s})} \cdot \frac{(V_{Bc} / (m^{3}/\text{kmol}) - V_{B} / (m^{3}/\text{kmol}))^{3/2}}{(V_{Bc} / (m^{3}/\text{kmol})^{4/3} (V_{Ac} / (m^{3}/\text{kmol}) - V_{A} / (m^{3}/\text{kmol}))^{1/2}}.$$
(24)

Many of the equations demand an estimate of molar volume of the solute and the solvent at the normal boiling point, which is not always easy to get, but it can be estimated from atomic increments. For polar components, the value of association factor is uncertain in the Wilke-Chang equation. Diffusivity in a highly viscous solution becomes low. Higher temperatures improve the diffusivities for two reasons: through the direct effect of temperature; and through the effect of temperature on viscosity. A critical comparison of 13 different correlations for liquid viscosities is provided by [23].

Infinite dilution diffusivities can be used for the cases in which the solutions are dilute. For high-yield systems, the diffusivity in an infinite dilution cannot directly be used, because the diffusivities in liquid-phase are basically concentration-dependent. The concentration dependency of the liquid diffusivity can be estimated from the (Eq. 25) [25]:

$$D_{A,B} = \left(D_{A,B}^{0}\right)^{x_{B}} \left(D_{B,A}^{0}\right)^{x_{A}} \alpha. \tag{25}$$

The thermodynamic activity correction ( $\alpha$ ) is not demanded if the product and reactant have almost similar chain lengths and infinite dilution diffusivities are not far away from each other. For solvent mixtures (m), the individual diffusivities of the solute can be estimated from the (Eq. 26) [26]:

$$D_{Am}\mu_m^{0.8} = \sum x_i D_{Ai}^0 \mu_i^{0.8}. {26}$$

### 8.3 Gas solubility

Gas solubilities are required for the evaluation of gas-liquid mass transfer fluxes. Although solubilities can be estimated from thermodynamic theories, a direct experimental approach is preferred. Henry's law is the standard way of describing the solubilities of sparingly soluble gases in liquids. Temperature-dependent empirical correlations for solubilities of many gases are available [27]. In the presence of electrolytes, the salting-out effect should be included (preferably according to the theory in [28]).

### 8.4 Thermal conductivity

Whenever an excessive amount of heat is generated and the reaction rates are temperature-dependent, a simultaneous solution of heat and mass balances is required. Conduction, convection and dispersion are the ways in which heat transfers. Since the conductivities of each phase may differ greatly from each other, the detailed heat conduction geometry becomes very complex and it is not included in the modeling. Instead, an effective conductivity for particles or the whole bed is used to simplify the conduction modeling. The effective conductivity within particles has often been expressed to be a function of the particle porosity and the conductivities of solid and liquid [29]. Effective conductivity of the whole bed must include the effect of gases as well.

Provided that the conductivity of the catalyst is close to the conductivity of the liquid, an average thermal conductivity works well in the calculation of heat transfer within particles. For regularly shaped particles, it allows the use of simple geometry, although the particles are porous and pore structures may be very complex. The assumption is that the pores are completely filled with liquid. Generally, within particles, most of the heat is conducted through the better conducting material. When metalbased supports are used, the conductivity of the support material may be superior to that of liquid. In some cases, however, the support is of a low-conductivity material (e.g. active carbon) and the conduction in the liquid dominates.

The bed conductivity is a function of the fluid conductivity, the solid conductivity and the bed void fraction as shown below ((Eq. 27)):

$$\lambda_B = \lambda_F (\lambda_S / \lambda_F)^{(1 - \varepsilon_B)}. \tag{27}$$

The effective conductivity is between dry and wet bed conductivities. Superficial velocities of liquid and gas have been observed to have an impact on the effective thermal conductivity. However, in lab-scale packed bed reactors under the low flow interaction regime, practically no promotion of effective conductivity by fluid flows is to be expected.

### 8.5 Reaction enthalpy

Heats of formation of individual components can be used as a basis when evaluating the reaction enthalpies. Another option is to use group contribution methods. Again, one potential alternative is to use heats of formations of resembling compounds.

## 9 Liquid flow effects

The phenomena related to liquid flow are summarized in Figure 6.

### Liquid flow 1. Flow direction (up/down) Upward: a) +Higher liquid hold-up. b) -More extensive backmixing. Downward: Gravity driven. 2. Chanelling & stagnant zones a) Both present when downward flow. b) Liquids selects the way of least resistance. c) Can be reduced by having small particles. 3. External wetting & wall flow a) Active sites reachable only if externally wetted. b) Wall flow and chanelling main reasons for partial external wetting. 4. Pressure drop a) Small particles, large velocities and high viscosity increse the $\Delta p$ . 5. Liquid hold-up a) Total, static (not moving), dynamic (flows), external = static + dynamic (=non-capillary). b) Small particles, rough surfaces, high liquid flowrate increase hold-up. c) Where does the reactions take place? In which part of liquid? To be specified.

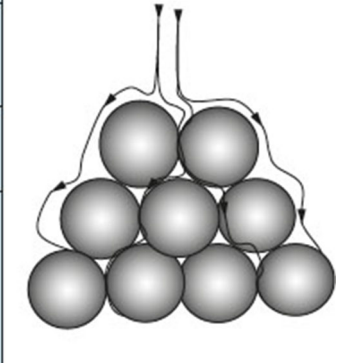


Figure 6: Flow-related phenomena in fixed beds [9].

### 9.1 Qualitative flow arrangement comparison

The co-current downward flow arrangement is the most typical selection for trickle bed reactors. Liquid flows down the external surfaces of the particles selecting freely flow paths of least resistance. Stagnant zones in between the particles may be generated. Compared to upward liquid flow arrangement, the advantages of a downward liquid flow are a lower extent of back-mixing and a lower pressure drop, whereas the disadvantage is a lower liquid hold-up (shorter mean residence time).

In the downward operating mode, liquid takes multiple paths of the lowest resistance, thus generating a residence time distribution. The stagnant liquid zones may produce a tail in this distribution. In a shallow reactor equipped with a fine feed distributor, the distribution becomes narrow. Channeling and catalyst bypassing can be avoided in lab-scale operation. In a lab-scale reactor, complete wetting can be approached by the combined effect of the fine sand bed feed distributor and the initial flooding procedure.

### 9.2 External wetting of the catalyst

Correlations are available to predict the external wetting efficiency [30]. The correlations are of a semi-empirical nature and they include parameters, the values of which have been optimized using original data. The correlations show correct trends and tendencies, but should be regarded as only indicative when starting to model a new system. The wetting efficiency is strongly liquid flow dependent. When parts of the external particle surface remain dry, it means that all the active sites in the pores of the dry section become unreachable to liquid reactants. The external wetting efficiency thus directly influences the catalyst effectiveness factor. In literature, incomplete wetting is discussed for most typical regular geometries, spherical and cylindrical shapes [31, 32], respectively.

### 9.3 Radial flow

Laboratory-scale trickle bed reactors operate quite close to the plug flow conditions. This means that the major concentration gradients are observed in the axial direction. Therefore, in mass balance based models the radial direction is frequently excluded. An experimental study of radial mass distribution in a larger scale reactor has been reported. There, the reactor bottom was divided into multiple annuli-shaped sections, and the liquid flow from each section was measured. This way the wall flow and its' fraction of the total volume flow could be revealed. Wall flow effect is especially strong when the particle-to-reactor diameter ratio is not small enough. Particle shapes and physical properties of the fluids are among the other factors determining the extent of wall flow. The wall flow effect is reduced when the liquid surface tension is low and when the liquid density is high [12].

### 9.4 Pressure drop

**DE GRUYTER** 

The two-phase pressure drop can be calculated with the general pressure drop equation for a single gas-phase flow by using a two-phase flow friction factor, (Eq. 28). A collection of pressure drop correlations is given in a trickle bed review article [10]. As a selected example, Larachi's equation for the friction factor, (Eq. 28), is given below:

$$f = \frac{1}{\left(X_G (Re_L We_L)^{1/4}\right)^{3/2}} \left(31.3 + \frac{17.3}{\sqrt{X_G (Re_L We_L)^{1/4}}}\right),\tag{28}$$

$$X_G = \frac{w_G \sqrt{\rho_G}}{w_L \sqrt{\rho_L}},\tag{29}$$

Kilpiö et al.

$$Re_L = \frac{\rho_L w_L d_p}{\mu_L},\tag{30}$$

$$We_L = \frac{\rho_L w_L^2 d_p}{\sigma},\tag{31}$$

The friction factor depends on the Lochardt-Martinelli ratio as well as the Reynolds and Weber numbers of the liquid, Eqs. (28)–(31). The use of this equation is straight-forward. The real challenge is how to estimate all the physical properties under true process conditions. Especially, the surface tensions are often missing for multi-component systems. The equation above is tailor-made for the low interaction regime. If superficial flow velocities are low and the reactor short, the pressure drop becomes only a small fraction of the operating pressure. The pressure drop can also result in a decrease in productivity by indirectly lowering the partial pressure of the gas reactant.

More precise pressure drop estimates can possibly be obtained for a regular geometry by solving the mass and momentum balances simultaneously using CFD. For various flow regimes, a collection of semi-empirical pressure drop correlations is given in [10]. In one study [33], an extensive two-phase pressure drop database was used for teaching a neural network and in that way to obtain a semi-empirical model for pressure drops. The pressure drop then became a function of both gas and liquid Reynolds numbers, the Galileo number of liquid, densities, superficial velocities and mean residence times in both phases, porosity of the bed, liquid hold-up and length of the reactor, Eqs. (32)–(37) and the single phase pressure drop of liquid, which can be evaluated with Ergun equation (Eq. 38). All these variables are practically attainable. The equations are listed below:

$$\psi_L = \frac{\Delta p / \Delta z}{\rho_L g} + 1 = \left(\frac{\varepsilon_B}{\varepsilon_L}\right)^3 \left(\left(\frac{E_1 R e_L}{(1 - \varepsilon_B) G a_L}\right) + \left(\frac{E_2 R e_L^2}{(1 - \varepsilon_B)^2 G a_L}\right)\right),\tag{32}$$

$$\psi_G = \frac{\Delta p / \Delta z}{\rho_G g} + 1 = \left(\frac{\varepsilon_B}{\varepsilon_B - \varepsilon_L}\right)^3 \left(\left(\frac{E_1 R e_G}{(1 - \varepsilon_B) G a_G}\right) + \left(\frac{E_2 R e_G^2}{(1 - \varepsilon_B)^2 G a_G}\right)\right),\tag{33}$$

$$\psi_L = 1 + \frac{\rho_G}{\rho_L} (\psi_G - 1); (34)$$

$$Re_L = \frac{\rho_L w_L d_p}{\mu_L},\tag{35}$$

$$Ga_L = \frac{\rho_L g d_p^3 \varepsilon_B^3}{\mu_L^2 (1 - \varepsilon_B)},\tag{36}$$

$$Ga_G = \frac{\rho_G g d_p^3 \varepsilon_B^3}{\mu_G^2 (1 - \varepsilon_B)},\tag{37}$$

 $E_1$ ,  $E_2$  = constants of the Ergun equation.

The Ergun equation (single phase pressure drop):

$$\frac{\Delta p}{\Delta z} = E_1 \frac{\mu_L \dot{m}_L}{g \rho_L d_p} \frac{(1 - \varepsilon_B)}{\varepsilon_B^3} + E_2 \frac{\dot{m}_L}{g \rho_L d_p} \frac{(1 - \varepsilon_B)}{\varepsilon_B^3}.$$
 (38)

### 9.5 Liquid saturation (hold-up)

Perhaps the most natural way to specify the volumetric reaction rates is to express them on total external liquid hold-up basis. The capillary-liquid does not flow and is therefore not included. The liquid hold-up depends on the superficial liquid and gas velocities, the physical properties of the fluids and the properties of the bed and particles. For a new application, new parameter optimization is recommended.

The most popular liquid hold-up expressions are power laws of dimensionless numbers. Each dimensionless number is either an aspect ratio or ratio of characteristic forces faced by the liquid volume element. These ratios determine how much liquid is held in a fixed bed. Power laws are popular because they are practical, mathematically well-behaving functions and they are also scientifically acceptable. After all, it is true that forces generate the flows. The liquid hold-up correlations given here are taken from an extensive review article [10]. The liquid saturation (volume fraction of non-capillary liquid) equations are Eqs. (39)–(42):

Kohler-Richard equation (Eq. 39) [34]:

$$\beta_{nc} = 0.71 \left(\frac{a_v d_p}{\varepsilon_B}\right)^{0.65} \left(\frac{\rho_L^2 g d_p^3}{\mu_L^2}\right)^{-0.42} \left(\frac{\rho_L w_L d_p}{\mu_L}\right)^{0.53} \left(\frac{\rho_G w_G d_p}{\mu_G}\right)^{-0.31}.$$
 (39)

Ellman equation, (Eq. 40) [35]:

$$\log\left(\beta_{nc}\right) = -0.42X_G^{0.24} Re_L^{0.14} \left(\frac{a_v d_K}{1 - \varepsilon_B}\right)^{-0.163}.$$
 (40)

Wammes equations, Eqs. (41) and (42) [36], valid for low interaction regime,  $Re_L < 11$ , and no gas flow:

$$\beta_{nc} = 16.3 \left(\frac{\rho_L w_L d_p}{\mu_L}\right)^{0.36} \left(\frac{\rho_L^2 g d_p^3}{\mu_L^2}\right)^{-0.39},\tag{41}$$

$$\beta_{nc} = 3.8 \left( \frac{\rho_L w_L d_p}{\mu_L} \right)^{0.55} \left( \frac{\rho_L^2 g d_p^3}{\mu_I^2} \left( 1 + \frac{\Delta p}{\rho_L g \Delta z} \right) \right)^{-0.42} \left( \frac{a_v d_p}{\varepsilon_B} \right)^{0.65}. \tag{42}$$

Physical properties of fluids are more strongly temperature and less strongly pressure dependent (gas density being the exception). The liquid hold-up becomes simply a function of superficial velocities in nearly isothermally operating short reactors with a negligible pressure drop. The most strongly temperature dependent physical property is the liquid viscosity and change in it is the main reason why the liquid saturation depends on temperature. High hold-ups (with same bed volume fraction) are obtained with viscous liquids using small particles having rough surfaces.

In the first liquid saturation expression, (Eq. 39), the terms on the right hand side are the catalyst property term, one kind of Galileo number and Reynolds numbers of liquid and gas. This equation has five parameters. At a constant temperature and pressure, this equation becomes a function of superficial velocities of liquid and gas only and then the total number of parameters is reduced to three. Since new reaction systems and operation conditions differ from the original ones, the original values are only indicative.

The liquid hold-up has been studied at very low liquid and gas velocities [37]. For their system, the liquid saturation became a function of mainly the Reynolds number of liquid and the particle-to-reactor diameter ratio. The total hold-up turned out to be almost constant, 0.4, and the static hold-up 0.1.

With CFD, there are two ways for modeling the liquid holdup. The first one is to model it with the porous media concept (without giving the detailed geometry at all), and the other is a free surface model based on

giving the detailed geometry. The porous media concept has been reported to be successfully utilized for evaluating the total liquid hold-up and the pressure drop in the bed [38]. CFD with a simplified geometry as an input and a free surface model is the most sophisticated and heaviest computational way to treat flow phenomena and could in principle be used for calculating the liquid hold-up (Lopes *et al.* 2007) for a bed packed with equal-sized spheres. This kind of modeling suits best for cases where particles have regular shape and flow is laminar. When catalyst particles are sieve fractions of crushed particles, no simple geometry exists. CFD, while being highly successfully applied in single-phase applications, is still struggling in multi-phase applications. The tolerances easily obtainable for a single-phase flow are hard to reach in multi-phase applications.

## 10 Reactor modeling steps

### 10.1 Overview

An overview of the model development stage is given in Figure 7. The model development progresses gradually from simpler cases to more advanced ones. The verification task aims at checking that the individual parts of the program code work reliably.

### Modelling steps 1 Verification with simpler cases (Plug-flow unit, ideally stirred tank, only single reaction, few reactions, only mass balances, only heat balances, only heat conduction, particles of ideal shape, etc.). 2. Modelling of individual phenomenon separately a) Each phenomenon = research field of its own. b) Everything can not be included in full detail. c) One has to make decisions (what to include, in what degree of details). 3. Modelling of a simplified reaction system Often demands experimental data from simpler systems where some of the reactions are supressed. 4. Sensitivity studies prior to estimation (single variable) 5. Minimisation of number of parameters Narrowing of search ranges, starting with a model having fewer parameters and gradually adding more. 6. Improving identification (Modest identification study) 7. Parameter estimation

Figure 7: Modeling steps of laboratory-scale fixed bed reactors [9].

### 10.2 Selected modeling policy

When developing three-phase fixed bed reactor models, lots of phenomena are simultaneously present, and one has to make simplifications and decisions on how detailed one should be. In our modeling, decisions were made not to deeply progress into details of particle technology and fluid dynamics.

### 10.3 Studies of simplified reaction systems

Our modeling study of the direct synthesis of hydrogen peroxide shows how sometimes it is possible to study the intrinsic kinetics of a simplified reaction system separately. Direct decomposition and total decomposition reactions could be studied separately from other reactions. This allowed one to determine the hydrogen peroxide decomposition parameters independently and to divide the extensive parameter estimation to smaller sub-tasks.

### 10.4 Ways how to rule out phenomena by experimental design

By proper selections of process conditions and reactor set-up, most heat and mass transfer related phenomena can be ruled out in preliminary studies. For example, by deciding to work with dilute concentrations and a

short reactor, the effects of adsorption terms in the reaction equation can be suppressed. As a bonus, the effects of heat and mass transfer become suppressed as well. The effect of internal diffusion can be suppressed by using small catalyst particles. The intrinsic kinetics are revealed by studying them in a slurry reactor equipped with intensive mixing. The effects of impurities are avoided by working with pure solutions. Criteria of how to avoid the generation of serious temperature gradients have been presented in literature [8]. The severity of temperature effects directly depends on catalyst loading. The temperature gradients can be reduced by diluting the catalyst bed with inert particles. Internal heat transfer effects can be reduced in trickle bed operation by selecting to work with smaller particles, although at the expense of an increased pressure drop. By having support materials of high thermal conductivity, the bed works more isothermally. A common practice, especially in preliminary laboratory tests and catalyst screening studies, is to work with dilute streams – also to suppress temperature gradients.

### 10.5 Sensitivity studies

Sensitivity studies are performed for two reasons: first, in order to test and make sure that the program can operate reliably in broad ranges of variables; and, second, to get a feeling of how the system behaves and reacts to individual parameter changes.

## 11 Balances for the generic three-phase fixed bed model

### 11.1 Mass balances for gas, liquid and solid phases

The general model equations presented here are suitable for calculations of the time-dependent concentrations of all compounds and temperature at each location inside a trickle bed reactor. In particular, three different locations are taken into account: axial and radial position inside the reactor and position within each particle in every location of the packing. The compressed mass balances of the components in gas and liquid, here presented for fluid, are given in (Eq. 43). This mass balance states that the accumulation is a net effect of gasliquid mass transfer, convection, axial and radial dispersion and finally the mass flux to/from the particles (the last term is usually present only for liquid balances). This last term is necessary because the reactions are assumed to take place here within the solid catalyst particles.

$$\varepsilon_{F} \frac{\partial C_{i,F}}{\partial t} = \pm J_{GL} - \frac{\partial \left( w_{F} C_{i,F} \right)}{\partial z} + \varepsilon_{F} D_{z,F} \frac{\partial^{2} C_{i,F}}{\partial z^{2}} + \varepsilon_{F} D_{r,F} \left( \frac{\partial^{2} C_{i,F}}{\partial r^{2}} + \frac{1}{r} \frac{\partial C_{i,F}}{\partial r} \right) - \frac{D_{e,i} s}{R_{p}} \frac{\partial C_{i,S}}{\partial r_{p}} \bigg|_{r_{p=R_{p}}} \tag{43}$$

The mass balance for the solid phase, (Eq. 44) states that the accumulation of each component depends on the internal diffusion and reaction terms. The equations demand the effective diffusivities and rate equations to be known for each component. The adjustable surface shape factor, together with well-defined characteristic particle dimension, are required for taking the particle geometry into account. The shape factor, s, for an arbitrary geometry can be estimated using (Eq. 45).

$$\frac{\partial C_{i,s}}{\partial t} = \frac{D_{e,i}}{\varepsilon_p} \left( \frac{\partial^2 C_{i,s}}{\partial r_p^2} + \frac{s}{r_p} \frac{\partial C_{i,s}}{\partial r_p} \right) + \rho_{cat} \cdot \sum \left( v_{i,j} r_{i,j} \frac{\varepsilon_F}{\varepsilon_p} \right)$$
(44)

$$s + 1 = \left(R_p \cdot \frac{A_p}{V_p}\right) \tag{45}$$

### 11.2 Energy balances for gas-, liquid- and solid phases

The energy balances for fluids (gas and liquid), (Eq. 46), state that the heat accumulation is the consequence of convective heat flux, heat conduction to axial and radial directions, heat fluxes caused by axial and radial

dispersion, and the heat flux from the particles (last term for liquid only). Among the key parameters for a correct description of temperature fields inside the reactor are the effective conductivities to the radial and axial direction of the reactor tube. Since three phases are involved in heat conduction, it is always a challenge to find well representative values for trickle beds.

$$\frac{\partial T_F}{\partial t} = \frac{\pm H_{GL}}{\varepsilon_F \rho_F c_{p,F}} - \frac{\partial (w_F T_F)}{\partial z} + \left(\frac{\lambda_{z,F}}{\varepsilon_F \rho_F c_{p,F}} + D_{z,F}\right) \cdot \frac{\partial^2 T_F}{\partial z^2} + \left(\frac{\lambda_{r,F}}{\varepsilon_F \rho_F c_{p,F}} + D_{r,F}\right) \left(\frac{\partial^2 T_F}{\partial r^2} + \frac{1}{r} \frac{\partial T_F}{\partial r}\right) - \frac{\lambda_{ps}}{R_p \varepsilon_F \rho_F c_{p,F}} \frac{\partial T_S}{\partial r_p}\Big|_{r_{p=R_p}}.$$
(46)

The energy balance of the solid phase, (Eq. 47), states that heat accumulation is the net result of heat conduction to characteristic direction and heat generation by reactions. Here the challenge is to estimate the effective particle conductivity, to select representative values for characteristic particle radius and surface shape factor and to have an accurate description of the reaction kinetics.

$$\frac{\partial T_s}{\partial t} = \frac{\lambda_p}{\rho_{cat}c_{p,s}} \left( \frac{\partial^2 T_s}{\partial r_p^2} + \frac{s}{r_p} \cdot \frac{\partial T_s}{\partial r_p} \right) + \frac{1}{c_{p,s}} \frac{\varepsilon_F}{\varepsilon_p} \left( \sum r_j \left( -\Delta H_r \right) \right). \tag{47}$$

### 11.3 Boundary conditions

Since the system consisted of a collection of PDEs, it became crucially important to define proper initial and boundary conditions. Boundary conditions are listed in full details in Eqs. (48)–(67).

$$C_{i,F}|_{z=0} = C_{i,F}^{IN},$$
 (48)

$$T_F|_{z=0} = T_F^{IN}, (49)$$

$$\left. \frac{\partial C_{i,F}}{\partial z} \right|_{z=I} = 0, \tag{50}$$

$$\left. \frac{\partial T_F}{\partial z} \right|_{z=L} = 0,\tag{51}$$

$$\left. \frac{\partial C_{i,F}}{\partial r} \right|_{r=0} = 0, \tag{52}$$

$$\left. \frac{\partial T_F}{\partial r} \right|_{r=0} = 0, \tag{53}$$

$$\left. \frac{\partial C_{i,F}}{\partial r} \right|_{r=R} = 0, \tag{54}$$

$$-k_r \cdot \left. \frac{\partial T_F}{\partial r} \right|_{r=R} = h_w \cdot \left( T_F |_{r=R'} - T_W \right) \tag{55}$$

$$C_{i,s}|_{z=0} = C_{i,s}^{IN},$$
 (56)

$$T_s|_{z=0} = T_s^{IN},$$
 (57)

$$\left. \frac{\partial C_{i,s}}{\partial z} \right|_{z=L} = 0, \tag{58}$$

$$\left. \frac{\partial T_s}{\partial z} \right|_{z=L} = 0,\tag{59}$$

$$\left. \frac{\partial C_{i,s}}{\partial r} \right|_{r=0} = 0, \tag{60}$$

$$\left. \frac{\partial T_s}{\partial r} \right|_{r=0} = 0, \tag{61}$$

$$\left. \frac{\partial C_{i,s}}{\partial r} \right|_{r=R} = 0, \tag{62}$$

$$-k_r \cdot \left. \frac{\partial T_s}{\partial r} \right|_{r=R} = h_w \cdot \left( T_s |_{r=R} - T_w \right), \tag{63}$$

$$\left. \frac{\partial C_{i,s}}{\partial r_p} \right|_{r_n = 0} = 0,\tag{64}$$

$$\left. \frac{\partial T_s}{\partial r_p} \right|_{r_n = 0} = 0,\tag{65}$$

$$C_{i,s}|_{r_p = R_p} = C_{i,F},$$
 (66)

$$T_s|_{r_v = R_v} = T_F. (67)$$

Boundary conditions are the feed concentrations and temperature at the reactor inlet, axial derivatives of concentrations and temperature at zero at the reactor outlet, radial derivatives of concentration and temperature as zero at reactor center due to symmetry and at the reactor wall concentration derivatives as zero and only heat flux to jacket. Concerning the particles, the boundary conditions are liquid concentrations and liquid temperature at the surface, zero derivative of both concentration and temperature in the center of the particles due to symmetry. At the reactor outlet, they are called Danckwerts closed boundary conditions. Reactor inlet boundary conditions are plug flow conditions due to downward gravity driven feed flows.

### 11.4 Sub-model examples

The model equations can be considered to be general for trickle bed reactors, because by switching on/off several parameters or terms, it is possible to describe a wide range of sub-models. Here some cases are depicted.

- 1. Reduction of the number of phases: by simply switching off the mass transfer terms and properly adjusting hold-up, it is possible to reduce the number of the phases to produce two-phase models in gas-liquid or liquid-solid systems.
- 2. Isothermal/adiabatic system: the wall heat transfer parameter can be adjusted in order to regulate the right heat transfer of the fixed bed. Of course, the two extremes can be either an isothermal or an adiabatic reactor, simply by choosing an infinite or zero value for this parameter and having a negligible heat generation rate.
- 3. Axial dispersion model: the radial dispersion can be switched off by neglecting the relative terms.
- **4.** Laminar flow model: by adjusting the velocity field and switching of the dispersion terms, a laminar flow can be easily described.

It is clear, that the total number of sub-models is large because a big amount of terms is considered in the mass and heat balances, so the model equations can be considered general and a starting point for the description of experiments performed in fixed bed.

# 12 Axial dispersion modeling and experiments

### 12.1 Classical axial dispersion model

The axial dispersion coefficient for the fixed bed reactor can be obtained from experiments carried out with inert tracers, which implies that the diffusion term originating from reaction rates in (Eq. 68) becomes zero. Furthermore, if radial dispersion is negligible and the tracer remains in liquid phase, the equation for a liquid-phase tracer is

$$\frac{\partial C_{i,L}}{\partial t} = D_{a,L} \frac{\partial^2 C_{i,L}}{\partial z^2} - \frac{w_L}{\varepsilon_L} \frac{\partial C_{i,L}}{\partial z}.$$
 (68)

The step or impulse changes for tracer are used in all the axial dispersion experiments. The most natural selection for the tracer is to use a component that is originally present in the feed or product stream and which do not significantly change the physical properties of the solution.

The dimensionless Peclet number is obtained from the axial dispersion coefficient, (Eq. 69).

$$Pe = w_L L / D_{a.L}. (69)$$

## 12.2 Alternative modeling approaches for back-mixing

Some alternative modeling approaches have been proposed, for example the piston exchange model and modeling with neural networks. The piston exchange model is based on the solution of twice the mass balances, one for the dynamic part of liquid and the other for the static part of liquid [39]. The two parameters that the piston exchange model has are dynamic liquid fraction and united mass exchange coefficient between the dynamic and static part of the liquid. Combined dimensional analysis and neural network modeling was used for an extensive amount of data from the open literature for evaluating the *Pe* number with a semi-emphirical expression [40]. This model was claimed to be capable of predicting the axial dispersion coefficient better than any other tested model. The neural network model used the Reynolds number of liquid, the Eötvos number of liquid, the Galileo numbers of liquid and gas, wall factor and mixed Reynolds number as inputs. A collection of the equations from open literature for evaluating the axial dispersion coefficient for specified systems under specified operation conditions was also presented. The two key variables that were present in all these models were the superficial velocity of liquid and the diameter of particles.

# 13 Numerical strategies

### 13.1 Model classification

Most of the models consist of parabolic partial differential equations (PDEs) that are solved numerically. Some of the models are ordinary differential equations (ODEs), either initial value problems (IVP) or boundary value problems (BVP). The mathematical structures of the models are summarized in Table 1. For each kind of model, an appropriate numerical solution strategy should be selected. Some common and robust numerical methods are reviewed in this section.

Table 1: Models and their mathematical structures.

Fixed bed model	Mathematical structure
Concurrent, pseudo-homogeneous, steady state/dynamic	ODE (IVP or BVP) / PDE (IVP)
Countercurrent, pseudo-homogeneous, steady	ODE (BVP) / PDE (IVP)
state/dynamic	
Concurrent, heterogeneous, steady state/dynamic	ODE (IVP + BVP or BVP) / PDE (IVP)
Countercurrent, heterogeneous, steady state/dynamic	ODE (BVP) / PDE (IVP)

Table 1 was prepared for cases in which the model only takes one spatial co-ordinate into account. As the table reveals, most of the mathematical structures are partial differential equations, because the concentrations and temperatures are time and space-dependent. Ordinary differential equations are obtained for steady state models. They are boundary value problems in most cases because of axial and/or radial dispersion effects. The models of catalyst particles are boundary value problems if steady state conditions prevail; but under transient conditions, the catalyst particle models are initial value problems.

### 13.2 Benefits of dynamic models

Dynamic models are preferable for several reasons: dynamic, time-dependent models can describe the reactor dynamics and catalyst activity changes, and they can be solved in a more robust manner than steady state models. The boundary value problems appearing in the steady state models are often tricky to solve, because some kind of iterative approach is needed (shooting methods), or approximation functions must be used such as orthogonal polynomials, which leads to a set of non-linear equations.

### 13.3 Solvers and solution algorithms

The numerical mathematics in the solution of ordinary differential equations (ODE-IVP) are advanced, and very robust and efficient numerical algorithms, such as backward difference methods and semi-implicit Runge-Kutta methods, have been developed for stiff ODEs, which appear in chemical systems [4]. The stiffness of the ODE system is the key issue having two principal origins: the rates of the chemical reactions can vary very much because a system can comprise both very rapid and very slow reactions, and the stiffness can increase due to the discretization of the spatial coordinates in the porous pellet or in the reactor system.

Because many efficient algorithms have been developed for stiff ODEs, it is very attractive to transform the PDEs appearing in three-phase reactor models to ODEs by applying a discretization procedure on the spatial coordinate. In this way, a system of parabolic PDEs is transformed to a large set of ODEs (IVP), which can be solved with stiff ODE algorithms. The discretization can be done in several ways, the most common ones are discretization with finite differences (method of lines) and discretization with approximation functions, such as orthogonal collocation. Orthogonal collocation or finite element methods are in principle more accurate than finite differences, but the implementation of finite differences is easier. This implies that the method of lines with finite differences is very often used even in spite of its disadvantages.

### 13.4 Numerical method of lines

Both the dynamic mass and energy balances can be solved by applying the numerical method of lines [41]. In the numerical method of lines, the spatial derivatives (i.e. longitudinal and radial concentration and temperature gradients) are replaced by their finite difference approximations. The simplest way is to use two-point approximations for the first derivatives and three-point difference for the second derivatives. By doing so, each partial differential equation is reduced into a set of ordinary differential equations. The problem can thereafter be expressed as a set of ordinary differential equations for which reliable solvers are readily available. It is possible to choose different discretization methods, such as the central finite difference method, the backward finite difference method, the forward finite difference method, the orthogonal collocation or finite elements method. The choice of the right method is not trivial and sometimes can even lead to physically unrealistic solutions. For example, backward differences should be used for the plug flow terms and central differences for the diffusion and dispersion terms to obtain a correct numerical solution. The number of discretization steps for each direction defines the grid where the calculations are performed. A large number of elements lead to a more accurate solution, consequently increasing the execution time of the code, a fact that is extremely important in parameter estimations problems in which the reactor model is invoked even thousands of times. A compromise between execution time and accuracy must be chosen by defining the right number of discretization elements. Approximation order and polynomial degree parameters have a great influence on the accuracy of the solution overall in coarse grids in which only a small number of elements are used. Stiff ODE solvers [42], always adjust the duration of each time step freely; when it faces numerical challenges, it simply starts to use smaller and smaller time steps. Then a computation, which initially starts well, has a tendency to slow down.

### 13.5 Hoyos method for particles

A numerical calculation method for evaluating the steady state diffusion and heat conduction within a cylindrical or a hollow cylindrical particle to both axial and radial directions was given originally in [43]. This Hoyos method can be extended to become valid for other geometries by adjusting the surface shape factor and diffusion path length properly. The method can be extended to cover particles of different shapes and used even for a rough estimate evaluation of a much more complicated geometry by simply using the adjustable surface shape factor and diffusion path length to compensate for the geometry. From the viewpoint of numerical efficiency, orthogonal collocation on finite elements is a very superior method in obtaining concentration and temperature profiles in porous catalyst particles and layers.

### 13.6 Parameter optimization methods

Estimation of kinetic and transfer parameters from experimental data implies always a use of an optimization algorithm, because the optimal values of the parameters are searched. Mostly the Levenberg-Marquardt method [44] is frequently used in parameter estimation tasks. Always, prior to the estimation tasks, multiple simulation studies over the range of interest for each parameter should be conducted. This is done to reveal the concentration responses and their sensitivity *a priori* and also in order to make sure that the possible convergence troubles can be faced and solved in the simulation stage to avoid surprises from arising in the more time-consuming parameter estimation tasks. Convergence problems can be surmounted by finding the combinations of variables in the simulation stage that caused the trouble and reasons for that. With this kind of strategy, the estimations can be carried out without significant disturbances using still rather broad ranges of parameter values, selected based on experience gained from the multiple simulation stage. The target function for the optimization is usually the sum of the least square deviation between the experimental and calculated concentrations. Separate weighting factors can be given to each and every observation point. Modest software was used in the examples (Citral hydrogenation, direct synthesis of hydrogen peroxide) presented in this review [45]. It has built-in ordinary differential equation solvers, simulation, sensitivity analysis and optimization routines.

### 13.7 Parameter number reduction

The number of parameters in each optimization task should be minimized without decreasing the accuracy. For the phenomena that can be studied separately, this should be done. Tracer tests for revealing the magnitude of axial dispersion coefficient serve as an excellent example. In many cases, a single phenomenon can become different when it is studied alone. Then it is not absolutely correct first to study the effect separately and then to use the obtained parameters in context that is different. An often-discussed example of this is the issue whether or not the mass transfer should be studied alone in a fixed bed operating at trickling flow regime [21]. Extrapolation of flow-related phenomena of a fixed bed in the trickling flow regime to different gas and liquid flow ranges is risky [47].

# 14 Scale-up issues of fixed beds

### 14.1 Overview

Figure 8 summarizes the major issues that appear in the scale-up of continuous fixed bed reactors [2–7].

Scale-up	Lab scale	Industrial scale
1. Reactor	Small diameter, short	Large diameter, long
2. Catalyst particles	Small, irregular shapes, size distribution	Large, regular tailor made shapes, single size
3. Catalyst dilution	Provides residence time, Mild conditions	Higher loading preferred
4. Concentration range	Narrow, dilute	Broad, concentrated
5. Pressure drop	Negligible	Operation cost, aimed low
6. Feed distribution	Fine	Challenging
7. Chanelling and stagnant zones	Minor challenge	Hard to avoid
8. Radial T and C gradients	Mild	More severe
9. Internal diffusion	Controlled	More severe
10. Internal heat conduction	Minor challenge	May become a problem, hot spots
11 Liquid velocities	Low	Higher
12. Operation conditions	Global	Local
13. Axial dispersion	Present	Different

Figure 8: Scale-up issues [9].

### 14.2 Large scale operation

In large-scale operation, it is not as easy to avoid the generation of temperature and concentration gradients. One of the main reasons for this is that chemical industry prefers to work with concentrated streams to intensify the process. High pressure drop is not acceptable because it directly affects the operating costs. Therefore, large catalyst particles have to be used. Industry also pushes towards more compact reactor sizes. Then catalyst dilution is not desirable. Due to the large reactor diameter, even distribution of liquid feed (and also redistribution) becomes more challenging. Superficial velocities of gas and liquid are typically set at higher levels in industrial units. As a consequence of all these factors, industrial units typically work in many ways under more severe conditions, which makes the undesirable flow, heat and mass transfer phenomena to emerge.

### 14.3 Gradients in scale up

When temperature gradients arise in a trickle bed reactor, they normally appear first in a radial direction. The heat transfer area per unit volume becomes smaller, the larger the diameter of the reactor is required. Then one of the remaining options to decrease severe temperature gradients and to improve the radial heat recovery is to select a multi-tubular reactor. Axial temperature gradients become more severe if the radial heat cannot be effectively recovered. If the liquid flow is channeled and stagnant places do exist, uniform temperature is hard to get and hot spots can emerge.

### 14.4 Flow regime in scale-up

In the reactor scale-up, it is extremely important that also in the bigger scale, the reactor operates at the same flow regime. Otherwise, unexpected behavior may arise, since many of the flow-related phenomena are strongly flow-regime dependent. A lot of studies have been conducted to evaluate the borderlines between flow regimes. The type of flow regime depends on the magnitudes and the ratio of superficial gas and liquid velocities, the physical properties of the fluids involved and the properties of the catalyst bed. Flow maps do exist, but they are case specific and, therefore, mostly indicative. Both experimental correlations and semi-empirical expressions to figure out the flow regime can be found.

### 14.5 Back mixing in scale-up

The extent of axial dispersion in large-scale operations is hard to predict based on small-scale experiments alone. The real challenge in the scale-up using an axial dispersion model is faced when trying to figure out how to get an estimate of the axial dispersion coefficient for a large unit without large-scale experiments. The axial dispersion coefficient can hardly be kept constant in scale-up, since this single parameter takes into account all kinds of flow non-idealities, and the extent of these are strongly scale dependent.

## 15 Examples

### 15.1 Citral hydrogenation

The use of renewable raw materials instead of petroleum-based ones is one of the main research fields of green chemical processes for the future and is, therefore, studied intensively worldwide. An example from this field is the production of citronellal from citral, a renewable compound from essential oils. Citronellal is a key compound that can serve as a starting material for synthesis of a wide spectrum of organic compounds, the most famous of which is perhaps menthol. An extensive review of the organic compounds that can be synthesized from citronellal does exist [48].

The reaction system is a complex one, but under the experimental conditions used by us, the system could be described with two reactions only:

$$Citral + H_2 \rightarrow Citronellal;$$
  
Citronellal +  $H_2 \rightarrow Citronellol.$ 

This implies that the system is a consecutive reaction, in which the first hydrogenation dominates; citronellal was the main product, while citronellol was a side-product. The catalyst was supported by nickel. The reactor flowsheet is displayed in Figure 9.

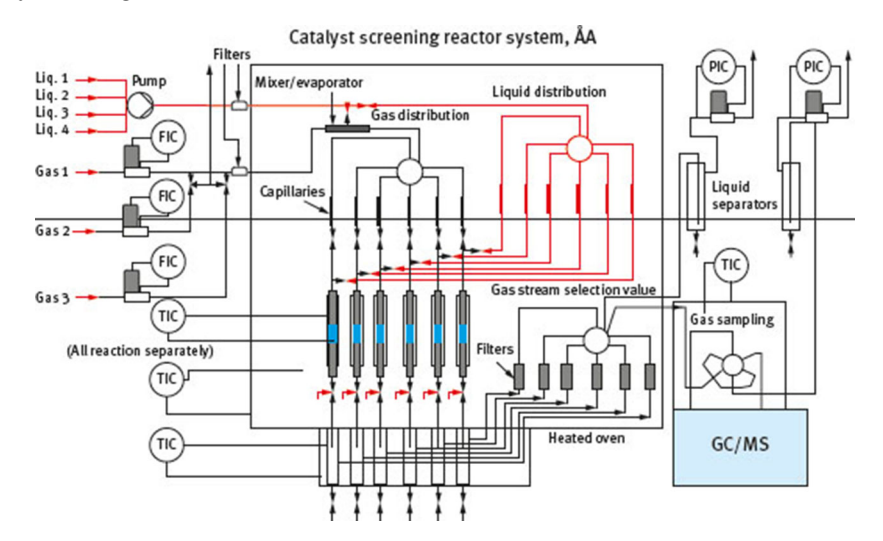
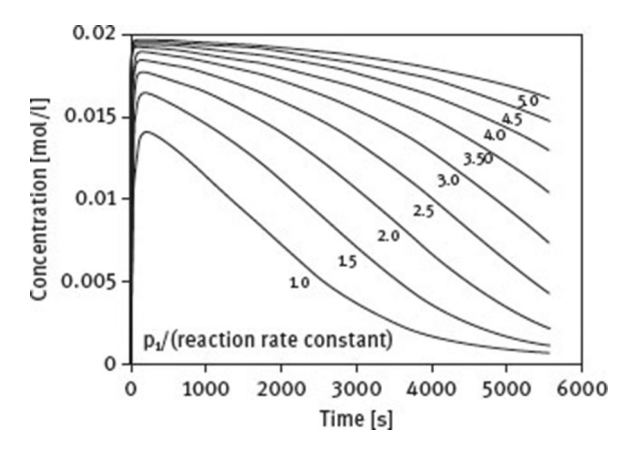
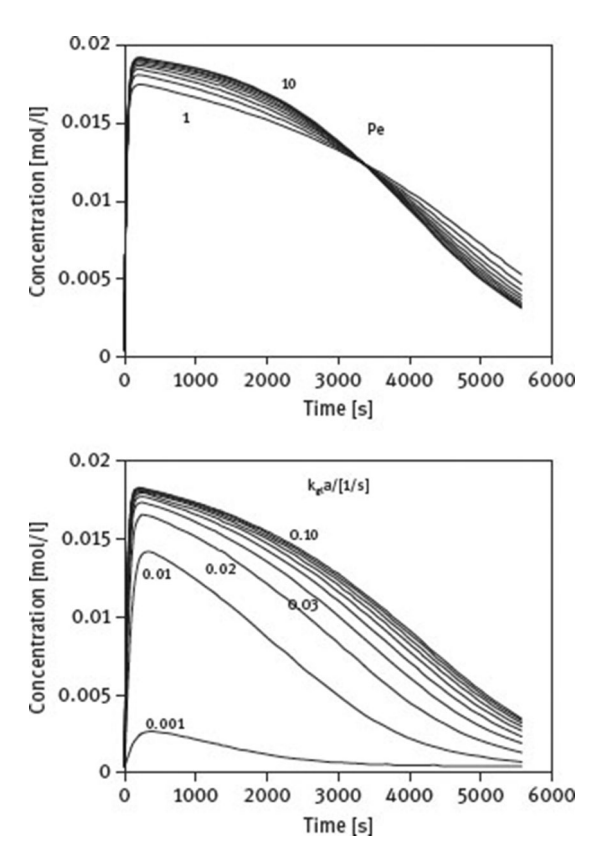


Figure 9: Experimental flowsheet for citral hydrogenation [49].

Figure 10 and Figure 11 present a set of results from the conducted sensitivity study. The sensitivity of the citronellal concentration on the changes of various key parameters is illustrated. The selected key parameters were: the reaction rate constant (in the absence and the presence of the deactivation), the gas-liquid mass transfer coefficient, the deactivation rate constant and the Peclet number. All the details of this study can be found from the corresponding article [46].



**Figure 10:** Example results from the sensitivity study. The effect of the reaction rate constant in the presence of catalyst deactivation [46]. Reprinted with permission from *Ind. Eng. Chem. Res.*, **2012**, *51* (26), pp. 8858–8866.



**Figure 11:** Example results from the sensitivity study. Effects of Peclet number and the gas-liquid mass-transfer coefficient on product concentration [46]. Reprinted with permission from *Ind. Eng. Chem. Res.*, **2012**, *51* (26), pp. 8858–8866 .

The final results of the parameter estimation study are given in Figure 12, which shows that the model very adequately describes the time-on-stream behavior of the citral hydrogenation system. The dominating effects for citral hydrogenation were the reaction kinetics along with the raw material dependent deactivation. The reaction system was very dilute, thus the mass transfer effects were suppressed.

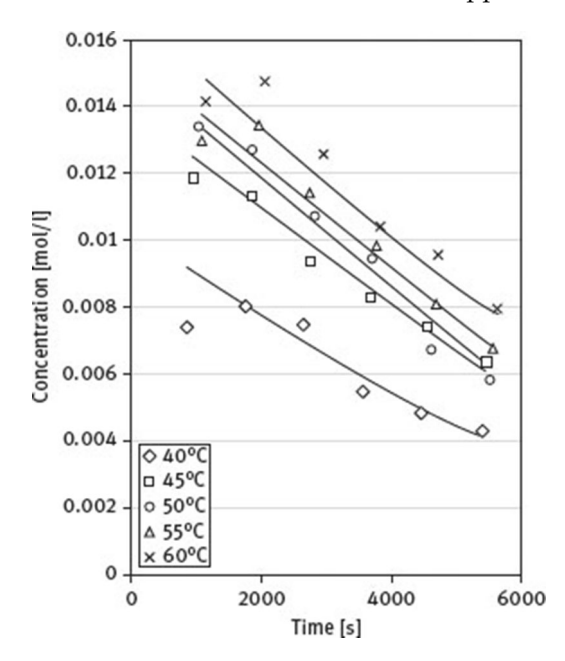


**Figure 12:** Example results from parameter estimation: citronellal concentration as a function of time-on-stream [46]. Reprinted with permission from *Ind. Eng. Chem. Res.*, **2012**, *51* (26), pp. 8858–8866 .

### 15.2 Direct synthesis of hydrogen peroxide

Hydrogen peroxide is a chemical component used in many industrial applications. It is used as a strong oxidant by the chemical industry and as a bleaching agent by the pulp and paper industry. With the conventional production technology, the anthraquinone process, hydrogen peroxide becomes relatively expensive. If hydrogen peroxide could be produced with a simpler process, it could be available with a more competitive price and could then be used more extensively in current and totally new applications.

Reviews that highlight the scientific community's pursuits to produce hydrogen peroxide in new ways exist [50, 51]. Direct synthesis from hydrogen and oxygen using a proper solvent and well-selected catalyst is one of the attractive alternatives. Direct synthesis in the presence of a Pd catalyst also served as our modeled example system. If it could be managed to be done safely with a catalyst exhibiting both high productivity and selectivity, the production process of this environmentally friendly

component could be essentially simplified. Due to the explosive nature of the  $H_2$  and  $O_2$  gas mixture, the direct synthesis experiments are usually carried out using a solvent. Methanol was used in our experiments. It was originally selected since, in the comparison of five potential solvents [51–53], methanol is mentioned as giving the highest rate of reaction. Our direct synthesis experiments were carried out outside the explosive regime. This implied that hydrogen content was low and, consequently, the gas-liquid mass transfer became also one issue of importance to be checked. The reaction system was a demanding one, since together with the desirable main reaction, also oxidation, direct decomposition and hydrogenation reactions took place, all leading to water formation. The system was experimentally studied under various superficial gas and liquid velocities and optimum velocity combinations had been observed both for the productivity and the selectivity viewpoints. In the experimental study, a very short reactor was used and the productivity in all the experiments was consequently low. Direct decomposition and total decomposition reactions were studied separately and modeled individually to improve the reliability of the model. The parallel-consecutive reaction system is displayed below in Figure 13.

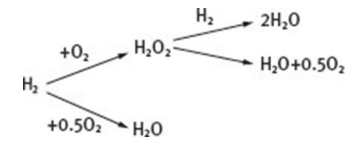
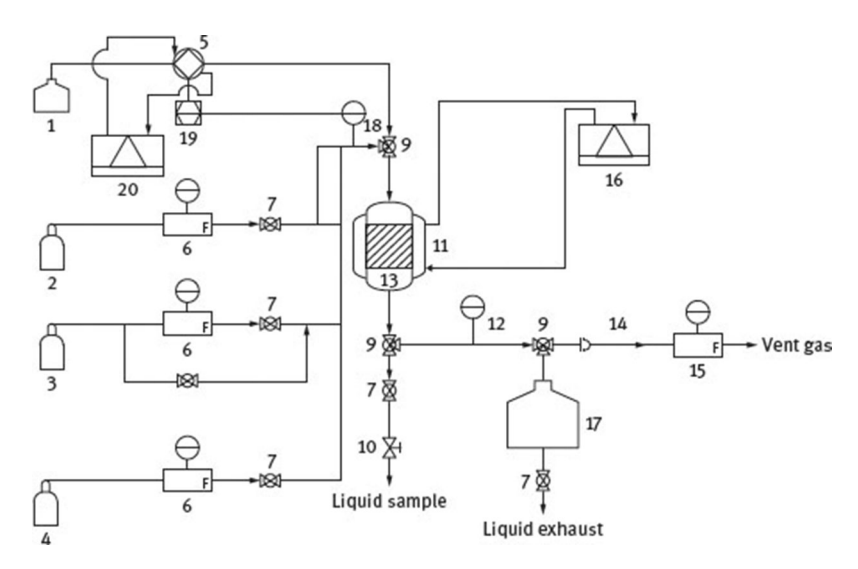


Figure 13: Reaction in direct synthesis of hydrogen peroxide.

The liquid hold-up parameters were optimized together with the kinetic parameters of the direct decomposition reaction by using direct decomposition data. Gas-liquid mass transfer parameters were estimated together with  $H_2O_2$  hydrogenation parameters using total decomposition data. Finally, synthesis and oxidation reaction parameters were estimated from the direct synthesis experiments when all the four reactions were taking place simultaneously. The modeling results of direct decomposition and total decomposition studies after the parameter estimation were in line with the experimental observations. The accuracy of the modeling results for the whole reaction system was improved by introducing an adaptive element to the model, namely a gas and liquid flow rate-dependent correction to all reactions. The flow range in the experimental studies of the  $H_2O_2$  decomposition was narrower than in the full reaction set studies. This might be one reason behind the observed deviations.

The reactor set-up is shown in Figure 14. The reactor was equipped with large inlet and outlet connections consisting of the pipelines and fine sand bed sections before and after the reaction section. Therefore, the whole reactor set-up approached plug flow behavior, Figure 15, although inside the reaction section, axial dispersion effects were clearly present. Details of the experimental axial dispersion studies and their numerical modeling can be found in article [47].



**Figure 14:** Fixed bed reactor set-up for direct synthesis of hydrogen peroxide [47]. Reprinted with permission from *Ind. Eng. Chem. Res.*, **2012**, *51* (41), pp. 13366–13378 .

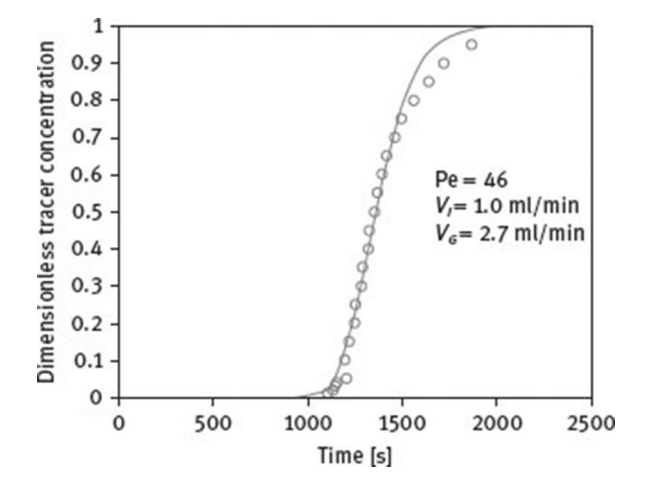


**Figure 15:** Tracer experiments and modeling: *Pe* number evaluation for the whole reactor [47]. Reprinted with permission from *Ind. Eng. Chem. Res.*, **2012**, *51* (41), pp. 13366–13378 .

The direct decomposition reaction was studied separately as a function of liquid and gas velocities. The parameter estimation results, Figure 16, show both the experimental data (points) and model predictions for various combinations of gas and liquid flow.

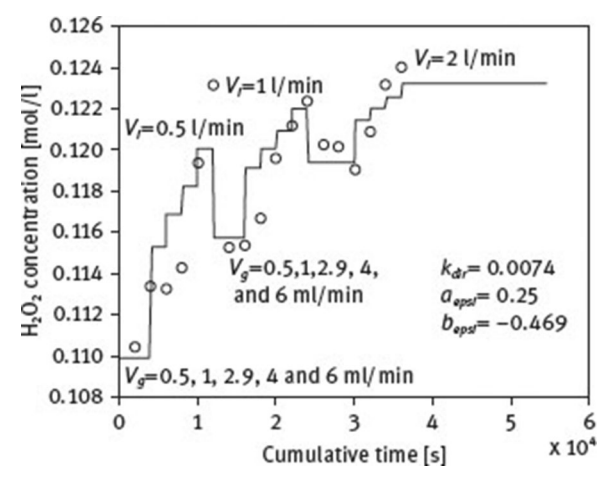


**Figure 16:** Parameter estimation results for the hydrogen peroxide decomposition study [47]. Reprinted with permission from *Ind. Eng. Chem. Res.*, **2012**, *51* (41), pp. 13366–13378 .

The parameter estimation for the case when all the four reactions were progressing was finally made in Figure 17. The results illustrate how closely the final model could follow the experimentally observed behavior.

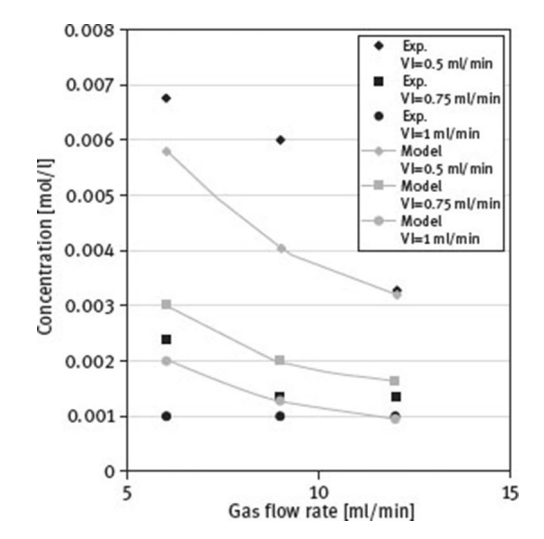


**Figure 17:** Parameter estimation results for the whole fixed bed reactor [47]. Reprinted with permission from *Ind. Eng. Chem. Res.*, **2012**, *51* (41), pp. 13366–13378 .

### 16 Conclusions

Design and modeling of laboratory-scale three-phase fixed bed reactors is a demanding task, comprising all the essential elements of chemical reaction engineering: thermodynamics, kinetics, fluid and catalyst properties, gas solubilities, mass and heat transfer effects and multiphase flow patterns. Recent advances in reactor technology, particularly the development of small and very precise experimental devices, with which several catalysts can be evaluated under varying conditions, implies a breakthrough in the efficiency of research efforts. Experimental data can be produced faster than ever. Experimental design becomes more important in order to keep the amount of experimental data within reasonable limits and to extract the best possible information. In order to progress in a rational way, these data should be systematically analyzed by mathematical modeling. In our opinion, the experimental data should be modeled based on physico-chemical theories, starting from the active site of the solid catalyst and ending up at the description of the flow behavior of the fixed bed reactor.

### **Acknowledgments**

The work is a part of the activities of Åbo Akademi Process Chemistry Centre (PCC), a center of excellence for scientific research. Financial support from the Academy of Finland is gratefully acknowledged.

This article is also available in: Saha, Catalytic Reactors. De Gruyter (2015), isbn 978-3-11-033296-4.

### References

- [1] Krishna R, Sie S. Strategies for multiphase reactor selection. Chem Eng Sci, 1994, 49, 4029–4065.
- [2] Froment G, Bishoff K. Chemical reactor analysis and design. New York, USA, John Wiley & Sons, 1979.
- [3] Levenspiel O. Chemical reaction engineering. New York, USA, John Wiley & Sons, 1999.
- [4] Salmi T, Mikkola JP, Wärnå J. Chemical reaction engineering and reactor technology. New York, USA, CRC Press, 2010.
- [5] Hagen J. Industrial catalysis, A practical approach, 2nd Edition, Weinheim, Germany, Wiley-VCH Verlag GmpH, 1999.
- [6] Belfiore L. Transport phenomena for chemical reactor design: New Jersey, USA, John Wiley & Sons, 2003.
- [7] Butt J. Reaction kinetics and reactor design: New York, USA, Marcel Dekker Inc., 2000.
- [8] Mederos F, Ancheyta J, Chen J. Review on criteria to ensure ideal behaviours in trickle-bed reactors. Applied catalysis A: General, 2009, 355, 1–19.
- [9] Kilpiö T. Mathematic modeling of laboratory scale three-phase fixed bed reactors. Thesis, Åbo, Finland, Åbo Akademi University, Department of Chemical Engineering, 2013.
- [10] Al-Dahhan M, Larachi F, Dudukovic M. Laurent A. High-pressure trickle bed reactors: A review. Ind Eng Chem Res, 1997, 36, 3292.
- [11] Leveneur S, Wärnå J, Salmi J, Murzin YM, Estel L. Interaction of intrinsic kinetics and internal mass transfer in porous ion-exchange catalysts: Green synthesis of percarboxylic acids. Chem Eng Sci, 2009, 64, 4101–4114.
- [12] Møller L, Halken C, Hansen J, Bartholdy J. Liquid and gas distribution in trickle-bed reactors. Ind Eng Chem Res, 1996, 35, 926–930.

- [13] Tukac V, Simickova M. Chyba V, Lederer J, Kolena J, Hanika J, Jiricny V, Stanek V, Stavarek P. The behaviour of pilot trickle-bed reactor under periodic operation. Chem Eng Sci, 2007, 62, 4891–4895.
- [14] Murzin D, Salmi T. Catalytic kinetics, ISBN: 0-444-51605-0, Amsterdam, Netherlands, Elsevier, 2005.
- [15] Mikkola JP, Salmi, T, Sjöholm, R. Modelling of kinetics and mass transfer in the hydrogenation of xylose over Raney nickel catalyst. J Chem Technol Biotechnol, 1999, 74, 655–662.
- [16] Salmi T, Murzin DY, Mikkola JP, Wärnå J, Mäki-Arvela P, Toukoniitty E, Toppinen S. Advanced kinetic concepts and experimental methods for catalytic three-phase processes. Ind Eng Chem Res 2004, 43, 4540–4550.
- [17] Cabrera MI, Grau, RJ. J Mol Catal A Chem, 287, 2008, 24.
- [18] Cabrera MI, Grau RJ. Trends in Chemical Engineering, 39–53, 2008.
- [19] Metaxas K, Papayannakos N. Gas-liquid mass transfer in a bench-scale trickle bed reactor used for benzene hydrogenation. Chemical Engineering & Technology, 2008, 31, 410–417.
- [20] Metaxas K, Papayannakos N. Kinetics and mass transfer of benzene hydrogenation in a trickle-bed reactor. Ind Eng Chem Res, 2006, 45, 7110–7111.
- [21] Koning B. Heat and mass transport in tubular fixed bed reactors at reacting and non-reacting conditions. Thesis, Twente, Holland, University of Twente, 2002.
- [22] Poling, B, Prausnitz, J, O'Connell J. Properties of gases and liquids. 5:th Ed. McGraw-Hill 2001.
- [23] Wild G, Charpentier, JC. Diffusivité des gaz dans les liquids, Paris, France, Techniques d'ingenieur, 1987.
- [24] Fei W, Bart HJ. Prediction of diffusivities in liquids. Chem Eng Technol, 1998, 21, 659–665.
- [25] Vignes A. Diffusion in binary solutions. Ind Eng Fundam, 1966, 5, 189–196.
- [26] Perkins LR, Geankoplis, CJ. Molecular diffusion in a ternary liquid with the diffusing component dilute. Chem Eng Sci, 1969, 24, 1035–1042.
- [27] Fogg P, Gerrard W. Solubility of gases in liquids, Chichester, England, Wiley, 1992.
- [28] Estimation of gas solubilities in salt solutions at temperatures from 273 to 363, AIChE ], 1996, 42, 298–300.
- [29] Woodside W, Messmer J. Thermal conductivity of porous media. I. unconsolidated sands. J Appl Phys 1961, 32, 1688.
- [30] Lappalainen K, Alopeus V, Manninen M, Aittamaa J. Improved hydrodynamic model for wetting efficiency, pressure drop and liquid holdup in trickle bed reactors. Ind Eng Chem Res, 2008, 47, 8436–8444.
- [31] Sakornwimon W, Sylvester, N. Effectiveness factors for partially wetted catalysts in trickle-bed reactors. Ind Eng Chem Process Des Dev,
- [32] Tsamatsoulis D, Papayannakos N. Partial wetting of cylindrical catalytic carriers in trickle-bed reactors. AIChE J, 1996, 42, 1853–1863.
- [33] Holub A. Thesis: Hydrodynamics of trickle bed reactors. Thesis, Washington, USA, Washington University, 1990.
- [34] Kohler M, Richarz W. Investigation of liquid hold-up in trickle bed reactors. Ger Chem Eng, 1985, 8, 295–300.
- [35] Ellman M, Midoux N, Wild G, Laurent A, Charpentier J. A new, improved liquid hold-up correlation for trickle-bed reactors. Chem Eng Sci, 45, 1677.
- [36] Wammes W, Mechielsen S, Westerterp K. The influence of pressure on the liquid hold-up in a cocurrent gas-liquid trickle-bed reactor operating at low gas velocities. Chem Eng Sci, 1991, 46, 409.
- [37] Lange, R, Schubert, M, Bauer T. Liquid hold-up in trickle bed reactors at very low liquid Reynolds numbers. Ind Eng Chem Res, 2005, 44, 6504–6508.
- [38] Atta A, Roy S, Nigam K. CFD of multiphase flow in high pressure trickle bed reactors: porous media concept, proceedings of European Congress of Chemical Engineering (ECCE-6). Copenhagen, 2007.
- [39] Stegeman D, van Rooijen F, Kamperman A, Weijer S, Westerterp, K. Residence time distribution in the liquid phase in a cocurrent gas-liquid trickle bed reactor. Ind Eng Chem Res, 1996, 35, 378–385.
- [40] Piche S, Larachi F, Iliuta I, Grandjean B. Improving the prediction of liquid back-mixing in trickle-bed reactors using a neural network approach. Journal of Chemical Technology and Biotechnology, 2002, 77, 989–998.
- [41] Schiesser W. The numerical method of lines: integration of partial differential equations. San Diego, California, USA, Academic Press, 1991.
- [42] Hindmarsh AC, ODEPACK-A Systematized Collection of ODE-Solvers. In: Stepleman R. Scientific Computing, Holland, IMACS/North Holland Publishing Company, 1983, 55–64.
- [43] Hoyos B, Cadavid J, Rangel H. Formulation and numeric calculation of non-Isothermal effectiveness factor for finite cylindrical catalysts with bi-dimensional diffusion. Latin American Applied Research, 2004, 34, 17.
- [44] Marquardt D. An algorithm for the least-squares estimation of nonlinear Parameters. SIAM Journal of Applied Mathematics, 1963, 11, 431–441.
- [45] Haario H. Modest user's guide. Profmath Oy, Helsinki, 2007.
- [46] Kilpiö T, Mäki-Arvela P, Rönnholm M, Sifontes V, Wärnå J, Salmi T. Modelling of a three-phase continuously operating isothermal packed-bed reactor: kinetics, mass-transfer, and dispersion effects in the hydrogenation of citral. Ind Eng Chem Res, 2012, 51, 8858–8866.
- [47] Kilpiö T, Biasi P, Bittante A, Salmi T, Wärnå J. Modelling of direct synthesis of hydrogen peroxide in a fixed bed reactor. Ind Eng Chem Res, 2012, 51, 13366–13378.
- [48] Leonardão E, Botteselle G, Azumbuja F, Perin G, Jacob R. Citronellal as key compound in organic synthesis. Tetrahedron 2007, 60, 6671–6712
- [49] Mäki-Arvela P, Eränen K, Alho K, Salmi T, Murzin D. Multi-tubular reactor design as an advanced screening tool for three-phase catalytic reactions. Topics in Catalysis, 2007, 45, 223.
- [50] Campos-Martin J, Blanco-Brieva G, Fierro J. Hydrogen peroxide synthesis: An outlook beyond the anthraquinone process. Angew Chem Int Ed, 2006, 45, 6962–6984.
- [51] Samanta C. Direct synthesis of hydrogen peroxide from hydrogen and oxygen: an overview of recent developments in the process. Applied Catalysis A: General 2008, 350, 133–149.

[52] Biasi P, Menegazzo F, Pinna F, Eränen K, Canu P, Salmi T. Hydrogen peroxide direct synthesis: Selectivity enhancement in a trickle bed reactor. Ind Eng Chem Res, 2010, 49, 10627–10632.

[53] Biasi P. Combination of catalyst development and chemical reaction engineering: a key aspect to improve the hydrogen peroxide direct synthesis. Doctoral Thesis, Laboratory of Industrial Chemistry and Reaction Engineering, Åbo Akademi University, 2013.